Research Article

iMedPub Journals
http://www.imedpub.com

Journal of In Silico & In Vitro Pharmacology

2022
Vol. 8 No. 5

DOI: 10.35841/2469-6692.8.5.11034

Targeting Oncogenic EGFR1, PI3 Kinase and BRAF: Identification of Multitarget Allosteric Kinase Inhibitors Using a Computational Methodology

Kavita Kumari Kakarala*, Kaiser Jamil

Department of Medicine, Bhagwan Mahavir Medical Research Centre, Hyderabad, Telangana, India

Corresponding author: Kavita Kumari Kakarala, Department of Medicine, Bhagwan Mahavir Medical Research Centre, Hyderabad, Telangana, India.

kavitakakarala@gmail.com

Citation: Kakarala KK, Jamil K (2022) Targeting Oncogenic EGFR1, PI3 Kinase & BRAF: Identification of Multitarget Allosteric Kinase Inhibitors Using a Computational Methodology. J In Silico In Vitro Pharmacol Vol.8 No.5:11034.

Abstract

Upregulation of EGFR1 activates several downstream signalling pathways, resulting in pathophysiological alterations that contribute to cancer. The RAS/RAF/MEK/ERK (MAPK) and PI3K/Akt/mTOR (PI3K/Akt/mTOR) pathways are major downstream signalling partners induced by EGFR1 activation. They play a crucial role in a variety of biological functions important for cell growth and proliferation. The alteration of these pathways and related pathogenesis has motivated the application of computer-aided targeting of this pathway to optimize therapeutic strategies targeting EGFR1, PI3K/Akt/mTOR and RAS/RAF/MEK/ERK (MAPK) signalling pathways. Several studies have demonstrated that computer-aided identification of new compounds has proven successful in drug development. To eliminate false negatives, this study used a pharmacophore and structure-based targeting method. The current study discovered multitarget allosteric inhibitors that target the crystal structures of EGFR1 (6DUK), PI3 Kinase (4A55), and BRAF kinase (6P3D). The current study was effective in identifying three small molecules: ZINC38783966, ZINC01456629, ZINC01456628 and 124173751, 137352549, 137353176, 137352399, 132020316 from ZINC and PubChem database respectively. It is interesting to note that the molecules ZINC38783966, ZINC01456628 and ZINC01456629, which are not yet annotated have shown high binding affinity with EGFR1 (6DUK), PI3Kinase (4A55) and BRAF (6P3D). A 50 ns molecular dynamics investigation also revealed that these potential novel multitarget kinase inhibitors had stable binding. Further, this study has also been able to identify targets for small molecules from the ZINC database, for which the annotation is not available yet..

Keywords: Kinase; Multitarget; Docking; Scoring; Free energy; Binding affinity; Drug like

Received: October 05, 2021, Manuscrfipft No. IPJSVP-21-11034; Editor Assigned date: June 03, 2022, PreQC No. IPJSVP-21-11034 (PQ); Reviewed date: June 13, 2022, QC No. IPJSVP-21-11034; Revised date: June 23, 2022, Manuscript No. IPJSVP-21-11034 (R); Published date: July 01, 2022, DOI: 10.35841/2469-6692.8.5.11034Upidi nim

Introduction

TThe metabolic pathways are coupled and work cooperatively. Signals received from the cell surface via receptors regulate their activation and deactivation. The multitude of proteins within the cell transmit and amplify the signal received from these receptors. The abnormal expression or activation of EGFR1 is associated with several human disorders, including immunological, neurological and infectious diseases. However, their role in cancer has received gained much attention [1-5]. The advances in the molecular mechanisms of cancer cell signalling, structural biology and bioinformatics established the role of kinases in causing cancer [6].

The epidermal growth factor receptor (EGFR1), PIK3CA and BRAF are three prominent oncogenic kinase therapeutic targets. PIK3CA activates major cancer cell signalling pathways and is linked to mutations and/or deletions in phosphatase and tensin homolog (PTEN), a phosphatase that negatively regulates PI3K [7-9]. EGFR1 is a transmembrane glycoprotein that modulates signalling pathways controlling cellular proliferation. The tyrosine kinase domain shows catalytic function. When EGFR1 binds to its ligand, intrinsic tyrosine/kinase activity autophosphorylates it, triggering a cascade of events that activate many signalling pathways. The activation of these downstream target sequences continuously and constitutively results in more aggressive tumour patterns. Overexpression of the EGFR1 gene can be due to EGFR1 gene amplification, endocytosis downregulation and induced ligand-independent interaction with the members of the same

ERBB family [10-13]. Altered expression of EGFR1 was correlated with a mutation of EGFR1 in 24.37% of all non-squamous non-small cell lung carcinoma patients. Although targeting EGFR1 in non-small cell lung cancer (NSCLC) has been beneficial, it is often discontinued due to drug resistance. Subsequently relapse of the disease occurs as EGFR1 overexpression is associated with the initiation of a cascade of events in which several proteins are involved (A total of 219 reactions and 322 species were included) [14]. The important pathways were ERK MAPK, PI3K-AKT, SRC, PLC-γ1-PKC, JNK, and JAK-STAT. These pathways crosstalk at various levels and propagate the signal to the entire network resulting in cell growth, proliferation, migration, and inhibition of apoptosis etc. [15].

Conserved kinase domain and allosteric inhibition

At least 518 protein kinases are encoded in the human genome [16]. 478 of them have catalytic domains that are well conserved. The remaining 40 proteins share similar folds of protein kinase, although they differ in sequence [17-19]. The catalytic domain and the ATP binding site in the active conformation of these TKs are remarkably similar. In addition, they share several short motifs, including high-glycine loop, conserved glutamate, gatekeeper domain, hinge region, and DFG motif as reviewed by Gazic and his colleagues [20].

Multitargeted allosteric inhibition therapy

PI3K/Akt/mTOR pathway and RAS/RAF/MEK/ERK (MAPK) pathways are some of the key signalling pathways which are induced by EGFR1 activation in cancer. The studies have shown that inhibition of certain components of the PI3K/Akt/mTOR pathway may slow down or even stop cancer growth or sensitize cancer cells to chemotherapy [21]. Interestingly, PI3Kα is known to be recruited and activated by epidermal growth factor receptor (EGFR1), a receptor tyrosine kinase (RTK), at the membrane [22]. While the other pathway RAS/RAF/MEK/ERK (MAPK) signalling cascade has been in focus for drug discovery, particularly RAF of this pathway has been targeted after the emergence of drug resistance and paradoxical activation upon inhibitor binding [23]. In cancer genomes, BRAF is a major target of oncogenic mutations and a single-point mutation, and V600E represents >90% of events [24]. Therefore, the RAF was thought to be an ideal drug target for drug development. The first generation of RAF inhibitors namely Vemurafenib, Dabrafenib and Encorafenib was developed, but their efficacy was compromised with drug resistance. The paradoxical activation upon inhibitor binding not only reduced their efficacy, but also induced secondary malignancies. Receptor tyrosine kinase signalling pathways are complicated, involving a variety of chemical mediators linked by many signal transduction pathways. As a result, blocking or inhibiting a specific target may be less successful in stopping cancer cell growth and proliferation. Monokinase inhibitors must therefore be replaced with drugs that target several targets. Targeting multiple kinases has a significant potency advantage due to the synergistic effect. Furthermore, because of the synergistic effect, this approach minimises the chance of developing drug resistance and may boost potency. Several multitarget agents have been designed as single kinase inhibitors and found to be multitarget inhibitors because of the structural homology among the ATP-binding site of kinases. Except in rare situations, such as some cases of chronic myeloid leukaemia, no patient can yet be cured by using receptor tyrosine kinase inhibitor (RTKI) as a single agent in the treatment. The primary difficulties for their usage in cancer patients are the emergence of treatment resistance and toxicity, which can lead to dose reductions or RTKI therapy termination. The toxic side effects are because they target ATP binding site which is physiologically important. Thus, targeting allosteric sites has emerged as one of the key approaches, where the inactive kinase conformation is stabilized. The use of allosteric inhibitors to inhibit activity of RAF is proposed in a recent review. Thus, use of multi- targeted therapy holds great promise for controlling these diseases and targeting allosteric sites may overcome drug resistance and toxicity of inhibitors.

Computational drug discovery; application in identifying potential allosteric multi-target small molecules

SBDD (Structure-based Drug Discovery) is already approved as a fast method for low-cost identification of leads. In addition, it has proven to be more effective than traditional drug discovery methods as it attempts to identify the molecular basis of a disease and leverages knowledge of the 3D structure of the biological target. Computational methods have been especially useful in the discovery of kinase inhibitors as reviewed by Gazic et al [25].

We aimed to break the chain of signal transduction across pathways in this study by discovering a multitarget inhibitor that binds to EGFR1, PI3, and BRAF kinase, three essential participants in the EGFR1 signalling cascade targeting allosteric sites. The goal of this research is to produce multiple-kinase drug regimens that target multiple sites in the pathways, reducing toxicity and drug resistance while achieving maximum synergistic effects.

Materials and Methods

System specifications: Processor Intel (R) Core (TM) i7-10750H CPU @ 2.60GHz, 2.59 GHz, RAM16.0 GB, Nvidia GEFORCE RTX 2060 graphic card was used (Figure 1).

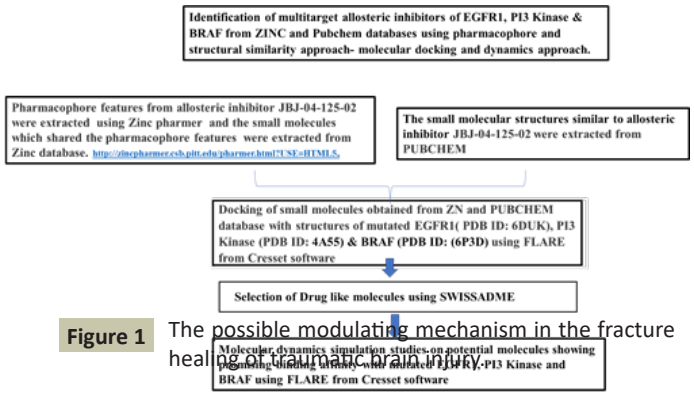

Figure 1 The possible modulating mechanism in the fracture healing of traumatic brain injury

Extracting Pharmacophore features of recent allosteric inhibitor JBJ-04-125-02 and identification of small molecules with similar pharmacophore features from ZINC and PubChem database.

ZINCPHARMER was used to extract a target-based pharmacophore

based on an allosteric inhibitor bound to JBJ-04-125-02. Target-based construction of pharmacophores takes account of the atomic interactions at the putative binding site of the target protein. Pharmacophore features were deduced from the geometry and interactions of the ligand bound to the target protein using 2 hydrogen bond donor/acceptor feature with coordinates x=37.95, y 89.84, z=-64.60; x= 37.04, y= 90.10, z= -66.77 and hydrophobic features coordinates x =37.51, y= 85.05, z = -62.58. 3272 molecules were derived from the ZINC database with the above descriptors.

Protein and Ligand Preparation

Cresset's Flare programme was used for molecular docking studies. The ligands file was read in autodetect under full protonation mode and was further optimized and minimized in Cresset Flare software using minimize option at default settings. The target protein structures of mutated EGFR1 (6DUK), PI3 Kinase (4A55) and mutated BRAF Kinase (6P3D) were downloaded from the PDB database (www.rcsb.org) and protein preparation was carried out in the Flare module of cresset software at default settings. Flare, version 4.0, Cresset®, Litlington, Cambridgeshire, UK.

Molecular docking studies

Docking and scoring was performed using Flare, (Cresset®, Litlington, Cambridgeshire, UK). Molecular Docking in Flare is based on the Lead Finder docking algorithm, Flare docking algorithm treats protein as rigid structure, and explores the possible conformations of the ligand around each freely rotatable bond. The final set of prepared 3272 molecules (section 2.1) obtained from ZINC PHARMER and 80 ligands from PubChem was docked with the EGFR1 (PDB ID-6DUK), PI3 kinase (PDB ID-4A55), BRAF (PDB ID-6P3D). The grid was positioned based on the active site residues reported or allosteric pocket identified: The residues 840-845, 699-715, and 115-123 comprise the allosteric pocket of PI3kinase (PDB ID-4A55) and the kinase domain is from amino acid residue 697- 1068. The residues D855, F856, E865 and K745 were selected as allosteric residues in EGFR1 structure of EGFR1 (PDB-6DUK) used for docking while in the crystal structure of BRAF (PDB-6P3D) H575, I573, D594, F595 were selected for grid generation. After grid generation docking was carried out with the ligands selected (refer section 2.1) using Flare™ V4 in Normal mode. Finally, the docked poses were scored using Lead Finder's scoring functions (Lead Finder, version, BioMolTech®, Toronto, Ontario, Canada). Flare software was used to analyse the docking performance [26]. Flare™ V4., Cresset®, Litlington, Cambridgeshire, UK). The interactions were also analysed using Maestro free viewer and Lig plot (Schrodinger Release 2021-1: Maestro, Schrödinger, LLC, New York, NY, 2021).

In Silico Druglikeness, Bioavailability, and Toxicology Prediction

Absorption, Distribution, Metabolism, Excretion/Elimination (ADME) evaluation of the compounds was carried out using SwissADME online software. To evaluate the pharmacokinetic properties of the compounds selected using ZINCPHARMER, SMILES (Simplified Molecular Input Line Entry System) chemical notation were entered in the interface of the website.

Molecular Dynamics studies of protein ligand complexes

Molecular dynamics simulation studies were carried out with selected EGFR1, PI3Kinase BRAF kinase ligand complex- for 50ns. The docked complex of ZINC-4A55 complex was simulated for 100ns to understand the stability of docked complex as the binding site is between two chains using Flare™ V4., Cresset®, Litlington, Cambridgeshire, UK. Molecular dynamics simulations in Flare are based on the OpenMM package. The supported small molecule force fields are AMBER/GAFF, AMBER/GAFF2 and Open Force Field. All the molecular dynamics simulations were carried out using AMBER FF14SB force field together with General Amber Force Field (GAFF) parameters [28]. The PDB file was loaded, OpenMM selected the GPU option by default, assigned Amber 14 forcefield parameters, and system was then explicitly solvated by using the TIP3P water model (Price and Brooks 2004). Subsequently, the system was modelled using topology information from the PDB file, the Long-range Coulomb interactions were calculated using the Particle Mesh Ewald (PME) method with a cut-off of 1 nanometre and the hydrogen bond length was constrained. Before starting molecular dynamics simulation, the system was energy minimized to eliminate clashes and then the system was simulated. Finally, the system was set for simulation using a Langevin integrator with a temperature of 300 K and a friction coefficient of 1 ps-1. Both 2 fs and 5 fs integration time stages were used in the simulations. The output was saved to a PDB file every 1000 steps. The structure was written in a DCD file, and the current time, potential energy, and temperature in a log file.

Results

Enormous funding was received for research on targeted therapy as an alternative strategy to chemotherapy for the treatment of cancer. However, the results were not encouraging after few months due to development of drug resistance. Some of the important reasons for the development of drug resistance are 1. Gene amplification 2. Inhibitors targeting conserved ATP binding site. 3. Activation of alternative pathways. Notably, most of the current EGFR1 TKIs target the ATP-site of the kinase, highlighting the need for therapeutic agents with alternative mechanisms of action, as the highest sequence and structural similarity across ATP pockets is an enormous obstacle for the specific inhibition of kinases. Consequently, targeting allosteric sites of kinases outside the extensively conversed ATP pocket was regarded as viable approach to circumvent present limitations of kinase inhibitors like poor selectiveness and drug resistance. To achieve significant inhibition, the downstream pathways that are activated and continue to trigger the activation of many more enzymes must also be controlled. Notably, PIK3CA, BRAF, and epidermal growth factor receptor (EGFR), are recognized as key oncogenic kinase drug targets, capable of activating significant tumor cell signaling pathways. Therefore, the present study attempted to identify novel multi-target inhibitors of EGFR1, PI3Kinase and BRAF kinase, which are the major sites of signal transduction in PI3K/AKT/mTOR and Ras/MEK/ERK pathways.

Multitarget allosteric inhibitors of EGFR1, PI3kinase, BRAF from ZINC database and PubChem Database

The three-dimensional structures of mutated EGFR1 (PDB ID 6DUK), PI3Kinase (4A55) and mutated BRAF (6P3D) were selected as they represent structures with bound allosteric inhibitors / known allosteric site, i.e. EGFR1 (6DUK) (Represents EGFR1 structure complexed with mutant-selective allosteric EGFR1 inhibitor, JBJ-04-125-02), PI3Kinase 4A55 (A non-ATP allosteric pocket was identified in a crystal structure of PI3K and BRAF (6P3D) The co-crystal structure of BRAF(V600E) with allosteric inhibitor ponatinib). Ponatinib binds to the BRAF dimer at an allosteric site and stabilizes a αC-helix conformation. EGFR1 is at the apex of the signalling cascade, and its activation results in the activation of more than 250 proteins. Therefore JBJ-04-125-02 an allosteric inhibitor, proved to inhibit EGFR1 phosphorylation using Ba/F3, H1975 and NIH-3T3 cells at a concentration of 0.01-10 μM and downstream AKT and ERK1/2 phosphorylation. Therefore, JBJ-04-125-02, which is a potent, mutant-selective, allosteric and orally active EGFR1 inhibitor with an IC50 of 0.26 nM targeting mutant EGFR1 L858R/T790M was selected for extracting pharmacophore features. The small molecules (3272) sharing the pharmcophoric features of allosteric EGFR1 inhibitor JBJ-04-125-02, and 80 ligands from Pubchem were docked into allosteric sites of crystal structures of EGFR1 (6DUK)I3Kinase (4A55) and BRAF(6P3D)using Flare, version 4.0, Cresset®, Litlington, Cambridgeshire, UK to identify multitarget allosteric inhibitors. The docked ligand conformations were generated treating protein as rigid structure and generating probable ligand conformations by moving functional groups around each freely rotatable bond. Flare is based on Lead Finder's docking engine. It combines a genetic algorithm search with local optimization processes, making it effective at coarse sampling of ligand poses and subsequent refinement of promising solutions. The output of docking calculations is represented with three distinct scoring functions. They are semi-empirical in nature and explicitly account for several kinds of molecular interactions. Empiric coefficients are applied to scale the individual energy contributions and generate three scoring functions. The Lead Finder offers three different scoring functions, Rank Score, dG score and VS score; Rank Score: It is optimized to allow an accurate prediction of 3D docked ligand poses, dG: It is optimized to provide an accurate estimate of the protein-ligand binding energy under the assumption that the pose is correct and VS: It is optimized for maximum efficiency in virtual screening experiments with maximum differentiation between active and inactive compounds in virtual screening experiments. dG-score gives an estimate of the free energy of protein -ligand binding. LF rank score indicates the ligand poses obtained during docking run. The LF score value provides highest score to the nearest experimentally observed ligand pose. LFVS assigns higher scores to the true binders of active ligands. Lead finder rank scores are mainly useful in ranking the docked ligand poses and is aimed to produce pose very close to experimentally observed ligand pose [29]. The results of docking studies with EGFR, PI3and BRAF kinase with molecules from ZINC database and PubChem Database was analysed (supplementary material S1-S6). The known inhibitors bound to the crystal structures were also docked along with the small molecules dataset to test the docking methodology. The allosteric molecules bound to crystal structures JBJ-04-125-02 (EGFR1-6DUK), P08 (PI3 Kinase-4A55) and 0LI 1001 (BRAF-6P3D) when docked gave following scores, LF rank score= -17.675 kcal/mol, -6.91kcal/mol, -18.326 kcal/mol and LFdG Score= -14.382 kcal/mol, -9.542 kcal/mol, -13.425 kcal/mol respectively (Table 1). The top 15 potential binders (Table 1, 2) were considered for further analysis.

Of the top 15 small molecules identified from ZINC database selected based on the LF scores, the molecules which showed potential for further evaluation as multitarget allosteric inhibitor targeting EGFR1, PI3Kinase and BRAF were as follows: ZINC38783966: (3S)-2-(1H-1,3-benzodiazol-2-yl) -5-methyl-4-[(naphthalen-1-yl) methyl]-2,3-dihydro-1H-pyrazol-3-ol with LF rank score= -16.244 kcal/mol and LF dG Score= -9.059 kcal/mol in EGFR1 (6DUK), LF Score= -15.374 kcal/mol, LFdG Score= -9.018 kcal/mol in PI3 kinase (4A55), LF Score=-14.122 kcal/mol, LFdG Score= -8.622kcal/mol in PI3kinase (6P3D) ;ZINC01456629: (1S,2S)-1,2-bis({1H-naphtho[2,3-d] imidazol-2-yl})ethane-1,2-diol with LF rank score= -15.942 kcal/mol; LFdG Score= -10.516 kcal/mol in EGFR1 (6DUK), LF Score= -15.365 kcal/mol LFdG Score= -8.174 kcal/mol in PI3 kinase (4A55); LF rank score= -15.182 kcal/mol, LFdG Score=-10.99kcal/mol in BRAF(6P3D); ZINC01456628: (1R,2R)-1,2-bis({1H-naphtho[2,3-d]imidazol-2-yl})ethane-1,2-diol with LF rank score= -15.777 kcal/mol, LFdG Score= -10.779 kcal/mol in EGFR1 (6DUK), LF rank score = -16.319 kcal/mol, LFdG Score= -9.602 kcal/mol in PI3 kinase (4A55), LF Score= -15.798 kcal/mol, LFdG Score = -10.46 kcal/mol in BRAF(6P3D). Further analysis showed that small molecules ZINC65548811 showed binding to EGFR1 and BRAF, and ZINC01866497 and ZINC3869007 showed binding to PI3Kinase and BRAF, while ZINC63281618 and ZINC00131302; ZINC64227798, ZINC64227784, ZINC64227795, ZINC64227785, ZINC39590767, ZINC38688875; ZINC63294896 showed high binding affinity only to EGFR1 (6DUK), PI3Kinase (4A55) and BRAF (6P3D) respectively.

This study was able to predict the binding affinity of some of the unannotated molecules in the ZINC database to different kinases studied. The kinase and molecules are as follows; EGFR1 (6DUK): ZINC38783966, ZINC59145547, ZINC63262046, ZINC01456629, ZINC01456628, ZINC63492708, ZINC63492706, ZINC64450349, ZINC39697225, ZINC65548811, ZINC63281618. PI3Kinase (4A55): ZINC01456628, ZINC01866497, ZINC38783966, ZINC64227784, ZINC64227795, ZINC64227785, ZINC39590767, ZINC39205099, ZINC63503139, ZINC63794402. ZINC39205096, ZINC38690079, ZINC38688875. BRAF (6P3D): ZINC01456628, ZINC01456629, ZINC03846543, ZINC38690079, ZINC39922313, ZINC65548811, ZINC38783966, ZINC01866497, ZINC63503138, ZINC63294896, ZINC39370775, ZINC63446186, ZINC63151227, ZINC38688873.

Among PubChem molecules the following molecules with compound ID 124173751, 137352549, 37353176, 137352399, 132020316 showed multitarget allosteric inhibition potential as they showed high binding affinity with EGFR1 (6DUK), PI3 Kinase (4A55) and BRAF (6P3D) respectively. The IUPAC names and the associated docking scores of the corresponding molecules with the respective protein structure was as follows: 124173751: (2R)-2-(5-fluoro-2-hydroxyphenyl)-2-[3-oxo-5-[4-(1-piperazinyl) phenyl]-1H-isoindol-2-yl]-N-(2-thiazolyl) acetamide, LF rank score= -19.928 kcal/mol, LFdG Score = -15.395 kcal/mol; 137352549: 2-[5-[2-(6-amino-3-pyridinyl)ethynyl]-4-methyl-3-oxo-1H-isoindol-2-yl]-2-(5-fluoro-2-hydroxyphenyl)-N-(2-thiazolyl)

Table 1 Potential multitarget allosteric binders identified from ZINC database (selected after pharmacophore (JBJ-04-125-02) based search of ZINC database using ZINCPHARMER) by docking against EGFR1 (6DUK), PI3K (4A55) and BRAF (6P3D)

	EGFR1 (6DUK)	PI3K (4A55)	BRAF (6P3D)
1	**6DUK -JBJ-04-125-02** (2R)-2-(5-Fluoro-2-hydroxyphenyl)-2-{1-oxo-6-[4-(piperazin-1-yl) phenyl]-1,3-dihydro-2H-isoindol-2-yl}-N-(1,3-thiazol-2-yl)acetamide LF rank score= -17.675 kcal/mol LFdG Score= -14.382 kcal/mol Ligand Interacting residues: F856 (π-π Interaction)	**4A55_P08 2063 (PI3K)** 6-methyl-2-morpholin-4-yl-8-[(1S)-1-phenylazanylethyl]chromen-4-one LF rank score= -6.91 LFdG Score = -9.542 kcal/mol Ligand Interacting residues: No bonded interactions observed	**A 0LI 1001** 3-(imidazo[1,2-b]pyridazin-3-ylethynyl)-4-methyl-N-{4-[(4-methylpiperazin-1-yl)methyl]-3-(trifluoro omethyl) phenyl}benzamide LF rank score= -18.326 kcal/mol LFdG Score= -13.425 kcal/mol Ligand Interacting residues: No bonded interactions observed
2	ZINC38783966 (1S,2S)-1,2-Bis(1H-benzo[f] benzimidazol-2-yl)ethane-1,2-diol LF rank score= -16.244 kcal/mol LFdG Score= -9.059 kcal/mol Ligand Interacting residues: Hydrogen bond interaction with D855	ZINC01456628 (1R,2R)-1,2-bis(1H-benzo[f] benzimidazol-2-yl)ethane-1,2-diol LF rank score =-16.319 kcal/mol LFdG Score=-9.602 kcal/mol Ligand Interacting residues: T908, Y904, F909 (π-π Interaction).	ZINC01456628 (1R,2R)-1,2-bis({1H-naphtho[2,3-d]imidazol-2-yl})ethane-1,2-diol LF Score=-15.798 kcal/mol LFdG Score =-10.46 Ligand Interacting residues: Hydrogen bond interaction with D594 This compound is not currently in any annotated catalogs.
3	**ZINC59145547** (2Z)-N-benzyl- 2-cyano-3-{4-[(1S)-5H-1lambda4,2,3,5-Thiatriazol -1-yl]- 3-nitrophenyl} prop-2-enamide LF rank score= -16.226 kcal/mol LFdG Score= -10.07 kcal/mol Ligand Interacting residues: Hydrogen bond interaction with K745, N842 and salt bridge with D855, D837	**ZINC01866497** [(3S)-5-(1-hydroxynaphthalen-2-yl)-3-phenyl-1,3-dihydropyrazol-2-yl]-phenylmethanone LF Score= -16.274 kcal/mol LFdG Score = -10.428 kcal/mol Ligand Interacting residues: Hydrogen bond interaction with F980 and π-π interaction with F989	**ZINC01456629** (1S,2S)-1,2-bis({1H-naphtho[2,3-d] imidazol-2-yl})ethane-1,2-diol LF rank score=-15.182 kcal/mol LFdG Score= -10.99 Ligand Interacting residues: Hydrogen bond interaction with E501
4	**ZINC63262046** (2E)-2- (2H-1,3-benzodiazol-2-yl) -3-[5-(2H-1,3-benzodiazol-2-ylsulfanyl)furan-2-yl]prop-2-enenitrile LF rank score= -16.033 LFdG Score=-10.344 Ligand Interacting residues: No bonded interactions observed	**ZINC01456629**(1S,2S)-1,2-bis(1H-benzo[f]benzimidazol-2-yl) ethane-1,2-diol LF Score=-15.365 kcal/mol LFdG Score=-8.174 Ligand Interacting residues: Hydrogen bond interaction with R951, F909, T908	**ZINC03846543** 4-hydroxy-3-[(5S)-5-(2-hydroxyphenyl)-4,5-dihydro-1H-pyrazol-3-yl]-1-methyl-1,2-dihydroquinolin-2-one LF rank score=-15.006 kcal/mol LFdG Score=-10.318 Ligand Interacting residues: Hydrogen bond interaction with E501 and D593
5	**ZINC01456629** (1S,2S)-1,2-bis({1H-naphtho[2,3-d] imidazol-2-yl}) ethane- 1,2-diol LF rank score= -15.942 kcal/mol LFdG Score= -10.516 kcal/mol Ligand Interacting residues: No bonded interactions observed	**ZINC64227798** (2S,5S,6S)-5-[(1R,9aS)-1H,2H,3H,4H,9aH-pyrido[3,4-b] indol-1-yl]-3-benzyl-2,6-dihydroxy-1,3-diazinan-4-one LF Score=-15.496 kcal/mol LFdG Score=-9.803 kcal/mol Ligand Interacting residues: Hydrogen bond interaction with C905, F909, Y985, and M1043	**ZINC38690079** 2-[(2E)-2-{[(3R)-1-[(2-fluorophenyl)methyl]-2,3-dihydro-1H-indol-3-yl]methylidene}hydrazin-1-yl]-2H-1,3-benzodiazole LF rank score=-14.891 kcal/mol LFdG Score=-9.195 Ligand Interacting residues: No bonded interactions observed

6	**ZINC01456628** (1R,2R)-1,2-bis({1H-naphtho[2,3-d]imidazol-2-yl})ethane-1,2-diol LF rank score=-15.777 kcal/mol LFdG Score=-10.779 Ligand Interacting residues: No bonded interactions observed	**ZINC38783966** (3S)-2-(1H-1,3-benzodiazol-2-yl)-5-methyl-4-[(naphthalen-1-yl) methyl]-2,3-dihydro-1H-pyrazol-3-ol LF Score=-15.374 kcal/mol LFdG Score=-9.018kcal/mol Ligand Interacting residues: π-π stacking interaction with Y985	**ZINC86863303** N,3-dihydroxy-N-(2-oxo-2,3-dihydro-1H-1,3-benzodiazol-5-yl) naphthalene-2-carboxamide LF rank score=-14.477 kcal/mol LFdG Score=-9.431 kcal/mol Ligand Interacting residues: Hydrogen bond interaction with D594, I527
7	**ZINC63492708** (3R)-2-(2H-1,3-benzodiazol-2-yl) -5-methyl-4-[(naphthalen-1 -yl)methyl]-2,3-dihydro-1H-pyrazol-3-ol LF rank score= -15.777 kcal/mol LFdG Score= -10.779 kcal/mol Ligand Interacting residues: Hydrogen bond interaction with K745, D855	**ZINC64227784** (2R,5S,6R)-5-[(1R,9aS)-1H,2H,3H,4H,9aH-pyrido (3,4-b] indol-1-yl]-3-benzyl-2,6-dihydroxy-1,3-diazinan-4-one LF Score=-15.128 kcal/mol LFdG Score= -10.369 Ligand Interacting residues: Hydrogen bond interaction with C905, T957, F909	**ZINC39922313** (2Z)-2-(2H-1,3-benzodiazol-2-yl)-3-[1-phenyl-3-(thiophen-2-yl)-1H-pyrazol-4-yl]prop-2-enenitrile LF Score=-14.346 kcal/mol LFdG Score=-10.736 Ligand Interacting residues: No bonded interactions observed
8	**ZINC63492706** (3)(3S)-2-(2H-1,3-benzodiazol-2-yl)-5-methyl-4-[(naphthalen-1-yl)methyl]-2,3-dihydro-1H-pyrazol-3-ol LF rank score= -15.367 kcal/mol LFdG Score=-7.915 Ligand Interacting residues: Hydrogen bond interaction with K745	**ZINC64227795**(2R,5S,6R)-5-[(1R,9aS)-1H,2H,3H,4H,9aH-pyrido[3,4-b]indol-1-yl]-3-benzyl-2,6-dihydroxy-1,3-diazinan-4-one LF Score=-15.099 kcal/mol LFdG Score=-10.084 Ligand Interacting residues: Hydrogen bond interaction with M1043 and C905	**ZINC65548811** 2-({[(5R)-1-(naphthalen-1-yl)-4,5-dihydro-1H-1,2,3,4-tetrazol-5-yl] sulfanyl}methyl)-2H-1,3- benzodiazole LF Score= -14.18 kcal/mol LFdG Score= -9.303 Ligand Interacting residues: Hydrogen bond interaction with E501
9	**ZINC64450349** 4-[(4S,7aR)-1-(2H-1,3-benzodiazol-2-yl)-3-methyl-6-oxo-1H,2H,4H,5H,6H,7H,7aH-pyrazolo[3,4-b]pyridin-4-yl]benzoic acid LF rank score=15.275 kcal/mol LFdG Score=-8.824 Ligand Interacting residues: No bonded interactions observed	**ZINC64227785** (2R,5S,6R)-5-[(1R,9aS)-1H,2H,3H,4H,9aH-pyrido[3,4-b] indol-1-yl]-3-benzyl-2,6-dihydroxy-1,3-diazinan-4-one LF Score= -14.933 LFdG Score=-10.547 Ligand Interacting residues: Hydrogen bond interaction with T957, F909 kcal/mol	**ZINC38783966** (3S)-2-(1H-1,3-benzodiazol-2-yl)-5-methyl4-[(naphthalen-1-yl) methyl]-2,3-dihydro-1H-pyrazol-3-ol LF Score=-14.122 kcal/mol LFdG Score=-8.622 Ligand Interacting residues: Hydrogen bond interaction with D594
10	**ZINC01020655** (1R)-1,4-diphenyl-2-(2-phenylethynyl)but-3-yne-1,2-diol LF rank score=-15.232 kcal/mol LFdG Score= -10.468 kcal/mol Ligand Interacting residues: Hydrogen bond interaction with F856	**ZINC39590767** (3S)-3-[(3S,7aS)-6-(4-methoxyphenyl)-1H,2H,3H,7aH-[1,2,4]triazolo[3,4-b] [1,3,4]thiadiazol-3-yl]-5-phenyl-3H-pyrazole LFdG Score= -9.76kcal/mol Ligand Interacting residues: Hydrogen bond interaction with T957, M1043 and C905	**ZINC01866497** 2-[(5S)-1-benzoyl-5-phenyl-2,5-dihydro-1H-pyrazol-3-yl]naphthalen-1-ol LF Score= -14.058 kcal/mol LFdG Score= -8.721kcal/mol Ligand Interacting residues: No bonded interactions observed
11	**ZINC13469899** [(1R,2S)-2-(5-cyano-1H-1,3-benzodiazol-2-yl)-1,2-dihydroxyethyl]-1H-1,3-benzodiazole-5-carbonitrile LF rank score=-14.958 kcal/mol LFdG Score= -9.344 Ligand Interacting residues: Hydrogen bond interaction with D837, A722	**ZINC39205099** 3-({[(3S,5R)-4,5-diphenyl-1,2,4-triazolidin-3-yl]sulfanyl}methyl)-1H-indole LF Score=-14.709 kcal/mol LFdG Score=-9.187kcal/mol Ligand Interacting residues: Hydrogen bond interaction with F909	**ZINC63503138-** ({[(3S, S)-4,5-diphenyl-1,2,4-triazolidin-3-yl]sulfanyl}methyl)-2H-indole LF Score=-13.849 kcal/mol LFdG Score=-10.197kcal/mol Ligand Interacting residues: Hydrogen bond interaction with E501, π- Cation interaction H574, K483

12	**ZINC39697225** (2E)-2-(2H-1,3-benzodiazol-2-yl)-3-(4-hydroxyphenyl)-1-phenyl-prop-2-en-1-one LF rank score=-14.732 kcal/mol LFdG Score= -9.801kcal/mol Ligand Interacting residues: Hydrogen bond interaction with K745	**ZINC63503139** 3-({[(3S,5R)-4,5-diphenyl-1,2,4-triazolidin-3-yl]sulfanyl}methyl)-2H-indole LF Score=-14.522 kcal/mol LFdG Score=-8. 822 kcal/mol Ligand Interacting Residues: Hydrogen bond interaction with M1043	**ZINC63294896** (3S,5R)-N-[(4-fluorophenyl)methyl]-3-[(2H-indol-3-yl)methyl]-1,2,4-oxadiazolidine-5-carboxamideLF Score=-13.808 kcal/mol LFdG Score=-9.226 kcal/mol Ligand Interacting residues: D594, E501,F595
13	**ZINC01020656** (1S)-1,4-diphenyl-2-(2-phenylethynyl)but-3-yne-1,2-diolLF rank score=-14.714 kcal/mol LFdG Score= -9.161 kcal/mol Ligand Interacting residues: Hydrogen bond interaction with D855, F856	**ZINC63794402** 2-[(3R)-4-[(2S)-1-methyl-2,3-dihydro-1H-1,3-benzodiazol-2-yl]-5-phenyl-3H-pyrazol-3-yl]phenolLF Score=-14.479 kcal/mol LFdG Score=-7.115 kcal/mol Ligand Interacting residues: No bonded interactions observed	**ZINC39370775** [4- methyl-3-(2-{2H-naphtho[2,3-d]imidazol-2-lsulfanyl} acetamido) phenyl] nitro}-lambda1-oxidanyl Ligand Interacting residues:LF Score=-13.769 kcal/mol LFdG Score=-8.495 kcal/mol
14	**ZINC65548811** 2-({[(5R)-1-(naphthalen-1-yl)-4,5-dihydro-1H-1,2,3,4-tetrazol-5-yl]sulfanyl}methyl)-2H-1,3-benzodiazole LF rank score=-14.612 kcal/mol LFdG Score= -7.457 kcal/mol Ligand Interacting residues: Hydrogen bond interaction with R841, N842	**ZINC39205096** 3-({[(3R,5S)-4,5-diphenyl-1,2,4-triazolidin-3-yl]sulfanyl}methyl)-1H-indoleLF Score=-14.479 kcal/mol LFdG Score=-9.35kcal/mol Ligand Interacting residues: Hydrogen bond interaction with T957	**ZINC63446186** [({1-phenyl-1H-pyrazolo[3,4-d] pyrimidin-4-yl}sulfanyl)methyl]-2H-1,3-benzodiazole LF Score=-13.715 kcal/mol LFdG Score=-8.571 kcal/mol Ligand Interacting residues: No bonded interactions observed
15	**ZINC63281618** (2S)-2-[(3S,7aS)-6-[(4-methoxyphenyl)methyl]-1H,2H,3H,7aH-[1,2,4]triazolo[3,4-b][1,3,4]thiadiazol-3-yl]-2H-indoleLF rank score=-14.52 kcal/mol LFdG Score= -6.938 kcal/mol Ligand Interacting residues: π-Cation interaction with K745	**ZINC38690079** 2-[(2E)-2-{[(3R)-1-[(2-fluorophenyl)methyl]-2,3-dihydro-1H-indol-3-yl]methylidene}hydrazin-1-yl]-2H-1,3-benzodiazoleLF Score=-14.466 kcal/mol LFdG Score=-8.448kcal/mol Ligand Interacting residues: No bonded interactions observed	**ZINC63151227** (1R,S)- 1,2-bis [(2R) -5-chloro -2H-1,3-benzodiazol- 2-yl]ethane-1,2-diol LF Score=-13.585 kcal/mol LFdG Score=-10.348 kcal/mol Ligand Interacting residues: No bonded Interactions observed
16	**ZINC71404923** (5S)-2-(4,5-dimethyl-1,3-thiazol-2-yl)-3,5-diphenyl-1,2,3,4-tetrazolidineLF rank score=-14.496 kcal/mol LFdG Score= -9.22 kcal/mol Ligand Interacting residues: K745	**ZINC38688875**- 2-({[(3S,5R) -4,5-diphenyl-1,2,4-triazolidin-3-yl] sulfanyl}methyl)-1H-1,3-benzodiazole LF Score=-14.158kcal/mol LFdG Score=-9.917kcal/mol Ligand Interacting residues: No bonded interactions observed	**ZINC38688873** 2-({[(3R,5R)-4,5-diphenyl-1,2,4-triazolidin-3- yl] sulfanyl} methyl)-1H-1,3-benzodiazoleLF Score=-13.468 kcal/mol LFdG Score=-9.398 Ligand Interacting residues: Hydrogen bond interaction with D504, E501,K483

acetamide, LF rank score= -19.249 kcal/mol, LFdG Score = -16.694 kcal/mol in EGFR1 (6DUK), LF rank score: -15.54 kcal/mol, LFdG Score: -13.622 kcal/mol in PI3Kinase (4A55); LF rank score = -13.129 kcal/mol, LFdG Score = -11.472 kcal/mol in BRAF;137353176 : 2-(5-fluoro-2-hydroxyphenyl)-2-[3-oxo-5-(2-pyridin-3-ylethynyl)-1H-isoindol-2-yl]-N-(1,3-thiazol-2-yl)acetamide-2-yl]-N-(1,3-thiazol-2-yl)propenamide LF rank score=-18.429 kcal/mol, LFdG Score =-13.726 kcal/mol in EGFR1(6DUK), LF rank score=-14.261 kcal/mol, LFdG Score=-11.062 kcal/mol in PI3 Kinase (4A55), LF rank score= -13.663 kcal/mol, LFdG Score=-10.359 kcal/mol in BRAF (6P3D);137352399: 2-[5-[2-(2-aminopyrimidin-5-yl) ethynyl]-3-oxo-1H-isoindol-2-yl]-2-(5-fluoro-2-hydroxyphenyl)-N-(1,3-thiazol-2-yl)acetamide LF rank score= -18.268 kcal/mol, LFdG Score =-13.84 kcal/mol in EGFR1(6DUK), LF rank score= -15.742 kcal/mol, LFdG Score= -13.123 kcal/mol in PI3Kinase (4A55), LF rank score= 14.208 kcal/mol, LFdG Score=-10.818 kcal/mol in BRAF (6P3D);132020316: 2-(5-fluoro-2-hydroxyphenyl)-2-[3-oxo-5-(4-piperazin-1-ylphenyl)-1H-isoindol-2-yl]-N-(1,3-thiazol-2-yl)acetamide LF rank score=-18.166 kcal/mol, LFdG Score=-14.612 kcal/mol in EGFR1(6DUK), LF rank score = -16.474 kcal/mol, LFdG Score = -12.348 kcal/mol in PI3 Kinase (4A55); LF rank score = -14.898 kcal/mol, LFdG Score = -11.7272 kcal/mol in BRAF (6P3D). While the molecules 132020315, 138534296, 135351618 showed binding affinity to only EGFR1 and PI3Kinase respectively. The molecules 124173751, 137353253, 147739925, and 146817163 showed potential binding to EGFR1and BRAF while small molecule 124173789 showed binding to PI3Kinase and BRAF (Table 2).

Table 2 : Potential binders of EGFR1 (6DUK), PI3K (4A55) and BRAF (6P3D) identified through docking studies with structurally similar small molecules with recent allosteric inhibitor of EGFR1 JBJ-04-125-02 from PubChem database.

S.No	EGFR1	PI3K	BRAF
1	JBJ_6DUK (2R)-2-(5-Fluoro-2-hydroxyphenyl)-2-{1-oxo-6-[4-(piperazin-1-yl) phenyl]-1,3-dihydro-2H-isoindol-2-yl}-N-(1,3-thiazol-2-yl) acetamide. LF rank score = -17.6 kcal/mol LFdG Score = -14.3 kcal/mol Ligand Interacting residues: No bonded interactions observed	**4A55_P08 2063** (PI3K) 6-methyl-2-morpholin-4-yl-8-[(1S)-1-phenylazanylethyl]chromen-4-one LF rank score= -6.91 LFdG Score = -9.542 kcal/mol Ligand Interacting residues: No bonded interactions observed	6P3D_A 0LI 1001_D (BRAF) 3-(2-imidazo[1,2-b] pyridazin-3-ylethynyl)-4-methyl-N-[4-[(4-methylpiperazin-1-yl) methyl]-3-(trifluoromethyl)phenyl]benzamide LF rank score = -18.326 kcal/mol LFdG Score = -13.425 kcal/mol Ligand Interacting residues: No bonded interactions observed
2	132020315 2-(5-fluoro-2-hydroxyphenyl)-2-[3-oxo-5-[4-(1-piperazinyl) phenyl]-1H-isoindol-2-yl]-N-(2-thiazolyl) acetamide;2,2,2-trifluoro-acetic acid LF rank score= -20.339 kcal/mol LFdG Score = -15.117 kcal/mol Ligand Interacting residues: D855, F856, K745, π-π interaction with F856	135351615 2-[5-fluoro-2-(hydroxymethyl) phenyl]-2-[3-oxo-6-(4-piperazin-1-ylphenyl)-1H-isoindol-2-yl]-N-(1,3-thiazol-2-yl) acetamide LF rank score= -16.765 kcal/mol LFdG Score= -12.575 kcal/mol Ligand Interacting residues: R951, R916, T908	132020316 5-fluoro-2-hydroxyphenyl)-2-[3-oxo-5-(4-piperazin-1-ylphenyl)-1H-isoindol-2-yl]-N-(1,3-thiazol-2-yl) acetamide LF rank score = -14.898 kcal/mol LFdG Score = -11.7272 kcal/mol Ligand Interacting residues: H574, K483 (π-cation)
3	124173751 (2R)-2-(5-fluoro-2-hydroxyphenyl)-2-[3-oxo-5-[4-(1-piperazinyl) phenyl]-1H-isoindol-2-yl]-N-(2-thiazolyl) acetamide LF rank score= -19.928 kcal/mol LFdG Score = -15.395 kcal/mol Ligand Interacting residues: D855, F856, E749, G865, E749	124173789 2-(5-fluoro-2-hydroxyphenyl)-2-[5-(1H-indol-5-yl)-3-oxo-1H-isoindol-2-yl]-N-(1,3-thiazol-2-yl) acetamide LF rank score= -16.687 kcal/mol LFdG Score= -8.28 kcal/mol Ligand Interacting residues: G1049, R95	124173789 2-(5-fluoro-2-hydroxyphenyl)-2-[5-(1H-indol-5-yl)-3-oxo-1H-isoindol-2-yl]-N-(1,3-thiazol-2-yl) acetamide LF rank score= -14.808 kcal/mol LFdG Score=-10.529 kcal/mol Ligand Interacting residues: A498, I592
4	137353253 2-[5-[2-(6-amino-3-pyridinyl) ethynyl]-3-oxo-1H-isoindol-2-yl]-2-(2-hydroxy phenyl)-N-(2-thiazolyl) acetamide LF rank score=-19.793 kcal/mol LFdG Score =-16.076 kcal/mol Ligand Interacting residues: D855, F856, L861, K745	132020316 2-(5-fluoro-2-hydroxyphenyl)-2-[3-oxo-5-(4-piperazin-1-ylphenyl) -1H-isoindol-2-yl]-N-(1,3-thiazol-2-yl) acetamide LF rank score = -16.474 kcal/mol LFdG Score = -12.348 kcal/mol Ligand Interacting residues: T957, F909	146817163 (2R)-2-(5-fluoro-2-hydroxy phenyl)-2-[3-oxo-5-(4-piperidin-1-ylphenyl)-1H-isoindol-2-yl]-N-(1,3-thiazol-2-yl) acetamide LF rank score= -14.739 kcal/mol LFdG Score= -11.355 kcal/mol Ligand Interacting residues: I573

5	138534296 (2R)-2-(5-fluoro-2-hydroxyphenyl)-2-[5-[4-(4-methyl-1-piperazinyl) phenyl]-3-oxo-1H-isoindol-2-yl]-N-(2-thiazolyl)acetamide LF rank score = -19.669 kcal/mol LFdG Score = -15.864 kcal/mol Ligand Interacting residues: D855, F856, E865	137352399 2-[5-[2-(2-aminopyrimidin-5-yl) ethynyl]-3-oxo-1H-isoindol-2-yl]-2-(5-fluoro-2-hydroxyphenyl)-N-(1,3-thiazol-2-yl) acetamide LF rank score= -15.742 kcal/mol LFdG Score= -13.123 kcal/mol Ligand Interacting residues: W1051, I913	137353217 2-(5-fluoro-2-hydroxyphenyl)-2-[3-oxo-5-(2-phenylethynyl)-1H-isoindol-2-yl]-N-(1,3-thiazol-2-yl) acetamide LF rank score= -14.531 kcal/mol LFdG Score=-10.88 kcal/mol Ligand Interacting residues: No bonded interactions observed
6	137352549 2-[5-[2-(6-amino-3-pyridinyl) ethynyl]-4-methyl-3-oxo-1H-isoindol-2-yl]-2-(5-fluoro-2-hydroxyphenyl)-N-(2-thiazolyl) acetamide LF rank score= -19.249 kcal/mol LFdG Score = -16.694 kcal/mol Ligand Interacting residues: K745, D855, F856, E865, E749	137352549 2-[5-[2-(6-aminopyridin-3-yl) ethynyl]-4-methyl-3-oxo-1H-isoindol-2-yl]-2-(5-fluoro-2-hydroxyphenyl)-N-(1,3-thiazol-2-yl) acetamide LF rank score: -15.54 kcal/mol LFdG Score: -13.622 kcal/mol Ligand Interacting residues: I913	137352399 2-[5-[2-(2-aminopyrimidin-5-yl) ethynyl]-3-oxo-1H-isoindol-2-yl]-2-(5-fluoro-2-hydroxyphenyl)-N-(1,3-thiazol-2-yl)acetamide LF rank score= 14.208 kcal/mol LFdG Score=-10.818 kcal/mol Ligand Interacting residues: I573
7	137352934 2-[5-[2-(6-amino-3-pyridinyl) ethynyl]-3-oxo-1H-isoindol-2-yl]-2-(5-fluoro-2-hydroxyphenyl)-N-(2-thiazolyl)acetamide LF rank score=-19.161 kcal/mol LFdG Score =-16.593 kcal/mol Ligand Interacting residues: No bonded interactions observed	139511888 4-[2-[1-(5-fluoro-2-hydroxyphenyl)-2-oxo-2-(1,3-thiazol-2-ylamino) ethyl]-3-oxo-1H-isoindol-5-yl] benzoic acid LF rank score= -15.462 kcal/mol LFdG Score= -12.354 kcal/mol Ligand Interacting residues: P984 (π-π interaction), R951, C905	137353176 2-(5-fluoro-2-hydroxyphenyl)-2-[3-oxo-5-(2-pyridin-3-ylethynyl)-1H-isoindol-2-yl]-N-(1,3-thiazol-2-yl) acetamide LF rank score= -14.135 kcal/mol LFdG Score= -9.837 kcal/mol Ligand Interacting residues: D576, D594, π-cation interaction-K483
8	147739925 2-(2-hydroxyphenyl)-2-[5-[6-[2-(methylamino) ethylamino]-3-pyridinyl]-3-oxo-1H-isoindol-2-yl]-N-(2-thiazolyl)acetamide LF rank score=-19.052 kcal/mol LFdG Score =-14.992 kcal/mol Ligand Interacting residues: K745, F856, D855, F856(π-π interaction) electrostatic interaction E865, E749	135351618 2-(5-fluoro-2-hydroxyphenyl)-2-(1-oxo-7-piperazin-1-yl-3H-benzo[e] isoindol-2-yl)-N-(1,3-thiazol-2-yl) acetamide LF rank score= -15.288 kcal/mol LFdG Score=-11.648 kcal/mol Ligand Interacting residues: R851, I913 π-π interaction with F954	124173751 (2R)-2-(5-fluoro-2-hydroxyphenyl)-2-[3-oxo-5-(4-piperazin-1-ylphenyl)-1H-isoindol-2-yl]-N-(1,3-thiazol-2-yl) acetamide LF rank score= -13.734 kcal/mol LFdG Score=-9.922 kcal/mol Ligand Interacting residues:H574, K483
9	135351618 2-(5-fluoro-2-hydroxyphenyl)-2-[1-oxo-7-(1-piperazinyl)-3H-benzo[e] isoindol-2-yl]-N-(2-thiazolyl) acetamide LF rank score= -18.663 kcal/mol LFdG Score = -14.442 kcal/mol Ligand Interacting residues: K745, F856, D855, F856(PI interaction) electrostatic interaction E865, E749	138534296 (2R)-2-(5-fluoro-2-hydroxyphenyl)-2-[5-[4-(4-methylpiperazin-1-yl) phenyl]-3-oxo-1H-isoindol-2-yl]-N-(1,3-thiazol-2-yl)acetamide LF rank score = -15.275 kcal/mol LFdG Score = -10.756 kcal/mol Ligand Interacting residues: R951, F909, T1025	135351676 2-(5-fluoro-2-hydroxyphenyl)-2-[3-oxo-5-(4-piperazin-1-ylphenyl)-1H-isoindol-2-yl]-N-(1,3-thiazol-2-yl) propenamide LF rank score= -13.663 kcal/mol LFdG Score=-10.359 kcal/mol Ligand Interacting residues: No Hydrogen bond interaction
10	137353176 2-(5-fluoro-2-hydroxyphenyl)-2-[3-oxo-5-[2-(3-pyridinyl) ethynyl]-1H-isoindol-2-yl]-N-(2-thiazolyl) acetamide LF rank score=-18.429 kcal/mol LFdG Score =-13.726 kcal/mol Ligand Interacting residues: K745, F856, D855	137353168 2-(5-fluoro-2-hydroxy phenyl)-2-[4-fluoro-3-oxo-5-(2-pyridin-3-ylethynyl)-1H-isoindol-2-yl]-N-(1,3-thiazol-2-yl) acetamide LF rank score= -14.693 kcal/mol LFdG Score=-11.053 kcal/mol Ligand Interacting residues:M1043	147739925 2-(2-hydroxyphenyl)-2-[5-[6-[2-(methylamino) ethylamino] pyridin-3-yl]-3-oxo-1H-isoindol-2-yl]-N-(1,3-thiazol-2-yl) acetamide LF rank score= -13.372 kcal/mol LFdG Score=-11.265 Ligand Interacting residues: His (π-cation), Ser 467, D594

11	137352399 2-[5-[2-(2-amino-5-pyrimidinyl) ethynyl]-3-oxo-1H-isoindol-2-yl]-2-(5-fluoro-2-hydroxyphenyl)-N-(2-thiazolyl) acetamide LF rank score= -18.268 kcal/mol LFdG Score =-13.84 kcal/mol Ligand Interactions: K745, F856, D855	139527951 (2R)-2-(5-fluoro-2-hydroxyphenyl)-2-(3-oxo-5-propan-2-yl-1H-isoindol-2-yl)-N-(1,3-thiazol-2-yl) acetamide LF rank score= -14.514 kcal/mol LFdG Score=-10.143 kcal/mol Ligand Interactions: No Hydrogen bond interaction	137353253 2-[5-[2-(6-amino-3-pyridinyl) ethynyl]-3-oxo-1H-isoindol-2-yl]-2-(2-hydroxyphenyl)-N-(2-thiazolyl) acetamide LF rank score = -13.361 kcal/mol LFdG Score = -11.908 kcal/mol Ligand Interactions: π-π cation studies K483, H574
12	132020316_D 2-(5-fluoro-2-hydroxyphenyl)-2-[3-oxo-5-(4-piperazin-1-ylphenyl)-1H-isoindol-2-yl]-N-(1,3-thiazol-2-yl) acetamide LF rank score=-18.166 kcal/mol LFdG Score=-14.612 kcal/mol Ligand Interacting residues: E749	138534364 2-(5-fluoro-2-hydroxyphenyl)-2-[5-[4-(4-methylpiperazin-1-yl) phenyl]-3-oxo-1H-isoindol-2-yl]-N-(1,3-thiazol-2-yl)acetamide LF rank score=-14.394 kcal/mol LFdG Score=-10.33 kcal/mol Ligand Interacting residues: Hydrogen bond interaction T908,pi cation interaction R951	139511888_D 4-[2-[1-(5-fluoro-2-hydroxyphenyl)-2-oxo-2-(1,3-thiazol-2-ylamino) ethyl]-3-oxo-1H-isoindol-5-yl] benzoic acid LF rank score = -13.288 kcal/mol LFdG Score = -9.714 kcal/mol Ligand Interacting residues: Hydrogen bond interaction D576
13	137353168_D 2-(5-fluoro-2-hydroxyphenyl)-2-[4-fluoro-3-oxo-5-(2-pyridin-3-ylethynyl)-1H-isoindol-2-yl]-N-(1,3-thiazol-2-yl)acetamide LF rank score= -17.845 kcal/mol LFdG Score= -13.789 kcal/mol Ligand Interacting residues: F856,D855,K745 Hydrogen bond interaction	137353176 2-(5-fluoro-2-hydroxyphenyl)-2-[3-oxo-5-(2-pyridin-3-ylethynyl)-1H-isoindol-2-yl]-N-(1,3-thiazol-2-yl) acetamide LF rank score=-14.261 kcal/mol LFdG Score=-11.062 kcal/mol Ligand Interacting residues: Hydrogen bond G1049, T972	137352549_D 2-[5-[2-(6-aminopyridin-3-yl) ethynyl]-4-methyl-3-oxo-1H-isoindol-2-yl]-2-(5-fluoro-2-hydroxyphenyl)-N-(1,3-thiazol-2-yl) acetamide LF rank score = -13.129 kcal/mol LFdG Score = -11.472 kcal/mol Ligand Interacting residues: Hydrogen Bond Interaction I573
14	139511888_D 4-[2-[1-(5-fluoro-2-hydroxyphenyl)-2-oxo-2-(1,3-thiazol-2-ylamino) ethyl]-3-oxo-1H-isoindol-5-yl] benzoic acid LF rank score=-16.656 kcal/mol LFdG Score=-13.657 kcal/mol Ligand Interacting residues:Ligand interaction=D855,F856	124173751_D (2R)-2-(5-fluoro-2-hydroxyphenyl)-2-[3-oxo-5-(4-piperazin-1-ylphenyl)-1H-isoindol-2-yl]-N-(1,3-thiazol-2-yl)acetamide LF rank score= -14.198 kcal/mol LFdG Score=-9.034 kcal/mol Ligand Interacting residues: Hydrogen bond T908,R916,R951.	137353168_D 2-(5-fluoro-2-hydroxyphenyl)-2-[4-fluoro-3-oxo-5-(2-pyridin-3-ylethynyl)-1H-isoindol-2-yl]-N-(1,3-thiazol-2-yl)acetamide LF rank score=-13.073 kcal/mol LFdG Score=-10.428 kcal/mol Ligand Interacting residues: Hydrogen bond interaction= H574
15	146817163_D (2R)-2-(5-fluoro-2-hydroxyphenyl)-2-[3-oxo-5-(4-piperidin-1-ylphenyl)-1H-isoindol-2-yl]-N-(1,3-thiazol-2-yl)acetamide LF rank score=-16.623 kcal/mol LFdG Score=-13.6577 kcal/mol Ligand Interacting residues: No bonded interactions observed	139527950_D 2-(5-fluoro-2-hydroxyphenyl)-2-(3-oxo-5-pentan-2-yl-1H-isoindol-2-yl)-N-(1,3-thiazol-2-yl)acetamide LF rank score=-14.005 kcal/mol LFdG Score=-10.168 kcal/mol Ligand Interacting residues: Hydrogen bond G1049, C905, R951	138534364_D 2-(5-fluoro-2-hydroxyphenyl)-2-[5-[4-(4-methylpiperazin-1-yl) phenyl]-3-oxo-1H-isoindol-2-yl]-N-(1,3-thiazol-2-yl)acetamide LF rank score=-12.92 kcal/mol LFdG Score=-9.388 kcal/mol Ligand Interacting residues: I573 and π cation interaction 575
16	135210254_D 2-(2-hydroxy-5-methylphenyl)-2-(5-methyl-3-oxo-1H-isoindol-2-yl)-N-(1,3-thiazol-2-yl)acetamide LF rank score=-16.13 kcal/mol LFdG Score=-16.13 kcal/mol Ligand Interacting residues: No bonded interactions observed	137353217_D 2-(5-fluoro-2-hydroxyphenyl)-2-[3-oxo-5-(2-phenylethynyl)-1H-isoindol-2-yl]-N-(1,3-thiazol-2-yl) acetamide LF rank score= -14 kcal/mol LFdG Score=-11.308 kcal/mol Ligand Interacting residues: No bonded interactions observed	135351618_D 2-(5-fluoro-2-hydroxyphenyl)-2-(1-oxo-7-piperazin-1-yl-3H-benzo[e] isoindol-2-yl)-N-(1,3-thiazol-2-yl) acetamide LF rank score=-12.919 kcal/mol LFdG Score=-9.401 kcal/mol Ligand Interacting residues: H574

Swiss ADME Analysis

In order to be effective as drug, small molecule must pass through an assessment of some of the properties like absorption, distribution, metabolism and excretion (ADME). In silico prediction of druglike properties from molecular structure is followed these days, as it saves lot of time and is economical. Additionally, it also reduces the failures in the drug development process. It is a tool for comprehensive analysis of various properties like physicochemical, pharmacokinetics, drug-likeness and medicinal chemistry feasibility. The results are displayed in the form Bioavailability Radar which is a snapshot of the important parameters checked by Swiss ADME. It is useful in understanding the drug likeliness of the molecule instantaneously. The pink area represents the optimum range for each property. The acceptable range of various parameters shown in the bioavailability radar are as follows; lipophilicity-XLOGP3 between −0.7 and +5.0, size, MW between 150 and 500 g/mol, polarity- TPSA between 20 and 130 A2, solubility-log S > 6, flexibility- > 9 rotatable bonds, saturation- fraction of carbons in the sp3 hybridization greater than or equal to 0.25. The drug likeness of the potential multitarget allosteric inhibitors of EGFR1 (6 DUK), PI3Kinase (4A55) and BRAF (6P3D) from ZINC database and PubChem database were analyzed using SwissADME tool for various properties like physicochemical, pharmacokinetics, drug-likeness and medicinal chemistry feasibility.

The oral bioavailability of compounds ZINC38783966, ZINC01456628 and ZINC01456629 showed one off-shoot relative to unsaturation (INSATU), which implies that they could have suboptimal physicochemical properties for their oral bioavailability. Further, small molecules ZINC38783966, ZINC01456628 and ZINC01456629 from ZINC Database and 124173751, 137352549, 137353176, 137352399 and 132020316 from PubChem database were predicted to be passively absorbed by the Gastrointestinal (GI) tract. ZINC38783966, showed blood-brain barrier (BBB) penetration, whereas the small molecules ZINC01456628 and ZINC01456629 from ZINC Database and 124173751, 137352549, 137353176, 137352399 and 132020316 from PubChem database compounds did not show BBB permeation. All the compounds were projected to be effluated from the central nervous system (CNS) by P-glycoprotein like crystal structure inhibitors (Fig. 2, Fig. 3 and Fig.4).

Figure 2

Swiss ADME analysis of potential candidates for multitarget allosteric drug targeting identified from Docking studies using FLARE from ZINC database. The bioavailability radar in each figure shows the various properties. The pink area is a suitable physicochemical space for oral bioavailability. The various properties depicted in bioavailability radar and their acceptable limits are as follows: Lipophilicity (LIPO): −0.7 < XLOGP3 < 5.0; SIZE: 150 g/mol < MW < 500 g/mol; polarity (POLAR): 20 A2 < topological polar surface area (TPSA) < 130 A2; and insolubility (INSOLU): 0 < LogS < 6; INSATU (insaturation): 0.25 < fraction of carbons in sp3 hybridization < 1; FLEX (flexibility): 0 < number of rotatable bonds < 9.

Figure 3 SwissADME analysis of potential candidates for multitarget allosteric drug targeting identified from Docking studies using FLARE from ZINC database. The bioavailability radar in each figure shows the various properties. The pink area is a suitable physicochemical space for oral bioavailability. The various properties depicted in bioavailability radar and their acceptable limits are as follows: Lipophilicity (LIPO): −0.7 < XLOGP3 < 5.0; SIZE: 150 g/mol < MW < 500 g/mol; polarity (POLAR): 20 A2 < topological polar surface area (TPSA) < 130 A2; and insolubility (INSOLU): 0 < LogS < 6; INSATU (insaturation): 0.25 < fraction of carbons in sp3 hybridization < 1; FLEX (flexibility): 0 < number of rotatable bonds < 9.

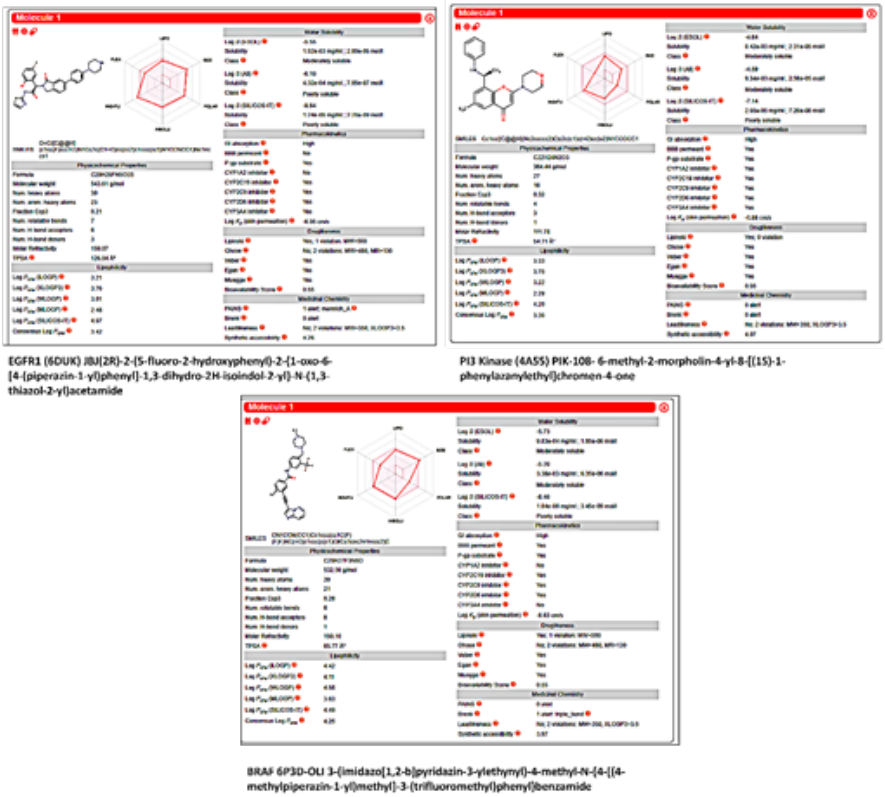

Figure 4 SwissADME analysis of the inhibitors bound to crystal structures OF EGFR1 (6DUK) -JBJ-04-125-02, PI3 Kinase (4A55)-PIK-108 and BRAF (6P3D)-OLI.

The role of metabolism in understanding the bioavailability of the drugs and drug–drug interactions is important. As Cytochrome P-450 enzymes (CYPs) interaction is important in predicting drug-likeness assessment and play a key role in drug-drug interaction study. Ten human CYPs from seven subfamilies, namely CYP1A2, CYP2A6, CYP2B6, CYP2C8, CYP2C9, CYP2C19, CYP2D6, CYP2E1, CYP3A4, and CYP3A5 are responsible for the metabolism of most drugs. The output of swissADME analysis of the potential molecules from ZINC and PubChem database was as follows: ZINC38783966 was predicted to inhibit CYP1A2, CYP2C19, CYP2C9 and CYP2D6; ZINC01456628 was predicted to inhibit CYP2C19 and CYP2D6; ZINC01456629 was predicted to inhibit CYP2C19, CYP2C9, CYP206. The small molecules from PubChem and the enzymes that were predicted to be inhibited were as follows; 124173751-CYP2C19, CYP2C9, CYP206, CYP3A4; 137352549- CYP2C9, CYP3A4; 137353176 -CYP2C9, CYP3A4; 137352399-CYP2C9, CYP3A4; and 132020316 - CYP2C9, CYP2C19 and CYP206. The predicted values for skin permeability coefficient (kp) were in the range of –5.19cm/s to –6.95cm/s. Further, the bioavailability score value of all the compounds was 0.55 (55%) indicating the probability of their bioavailability. Pan-Assay Interference compounds (PAINS) and BRENK filters were implemented to provide information regarding potentially challenging fragments (toxic, metabolically unstable, or possessing properties responsible for poor pharmacokinetics), in the chemical structures of compounds. Both filters showed no alert for ZINC38783966, ZINC01456628 and ZINC01456629, however one alert for pains and 0 alert for BRENK was shown for 124173751 and 132020316. 1 alert for BRENKS and PAINS was shown for molecules 137352549,137353176 and 137352399 respectively. Leadlikeness of the potential compounds was also calculated in addition to Lipinski's "rule of five" (Lipinski et al., 2001) and other four drug-likeness rules namely Ghose, Veber, Egan and Muegge were satisfied for ZINC38783966, ZINC01456628 and ZINC0145662, while Lipinski and Muegee rule of drug likeliness was satisfied for 124173751, 137352549, 137353176, 137352399 and 132020316. These properties were also analysed for the inhibitors in complex with crystal structures i.e. JBJ complex (2r)-2-(5-fluoro-2-hydroxyphenyl)-2-{1-oxo-6-[4-(piperazin-1-yl)phenyl]-1,3-dihydro-2h-isoindol-2-yl}-n-(1,3-thiazol-2-yl)acetamide EGFR1 (6DUK), OLI (3-(imidazo[1,2-b] pyridazin-3-ylethynyl)-4-methyl-n-{4-[(4-methylpiperazin-1-yl) methyl]-3-(trifluoromethyl)phenyl}benzamide) in PI3Kinase (4A55) complex, PIK-108 (6-methyl-2-morpholin-4-yl-8-[(1s)-1-phenylazanylethyl]chromen-4-one) in BRAF (6P3D) complex (Fig.4). The analysis showed high GI absorption, Bioavailability, lead likeness, synthetic feasibility, pharmacokinetics etc., like the drugs in complex with the crystal structures of the crystal structure inhibitor complex.

Considering their GI absorption, metabolism through CYPs, and drug-likeness, all of them could be excellent candidates for further studies and manipulations. Moreover, the calculations results showed that compound one was predicted not only to be not metabolized by CYPs, not permeate through BBB and be passively absorbed by GI tract, but also it had superior properties than other compounds in context to its lead-likeness (Figure 5).

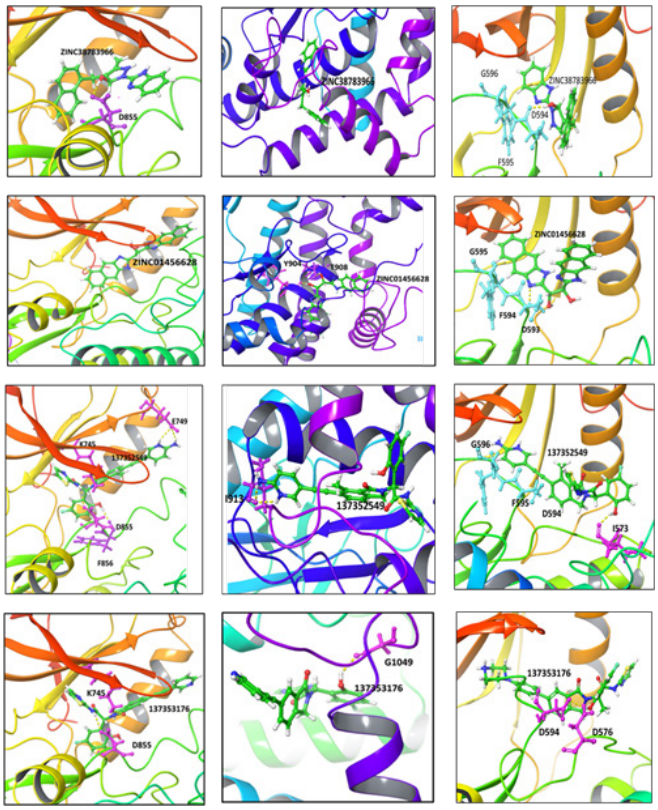

Figure 5 Binding pose of top 2 potential multitarget (EGFR1, PI3Kinase and BRAF) allosteric compounds from ZINC and PubChem database.

Ligand interaction studies

The amino acid residues involved in bonding interaction giving stability to the ligand in the binding pocket belonging to ZINC database were as follows: EGFR1 (6DUK) D855, K745, N842, D837, F856, A722 (hydrogen bond formation with the ligand) ; T908, Y904 ,Y985, M1043, C905, F909, R951, T957 (hydrogen bond formation with the ligand), F909, F980, F989, Y985 (π - π interaction) in PI3kinase: D594, E501, D593, D594, I527 (hydrogen bond formation with the ligand), in BRAF Kinase (Table 2, 3). Similarly, the key amino acid residue interactions observed in potential binders of PubChem database were as follows: EGFR1(6DUK): D855, F856, K745, E749, G865, E749, L861 (hydrogen bond interaction), F856 (π interaction); PI3 Kinase (4A55) R951, R916, T908, G1049, T957, F909, W1051, I913, C905, R851, T1025, M1043 (hydrogen bond interaction), P984 and F954 (π interaction); H574, A498, I592, I573, D576, D594, Ser 467 (hydrogen bond interaction), K483 (π-cation) in BRAF. Interestingly, the amino acid residues D855 (activation loop), K745 (Beta3 helix) in EGFR1 (6DUK); R9519 (activation loop), T908(alpha G), T957, F909 (alpha G), and M1043 in PI3 kinase (4A55) and H574, K483, Ser 46, D594, K483, in BRAF (6P3D) were the residues making key interactions with ligands belonging to both Zn and PubChem database.

Molecular Dynamics Simulation Studies

To understand the stability of binding affinity of the identified multitarget allosteric inhibitors, we performed molecular dynamics study on one of the promising small molecules from ZINC and PubChem database using FLARE. Conformational changes during protein–ligand interactions could be studied during MD simulations Molecular dynamics simulations in Flare are based on the OpenMM package. The detailed methodology is described in methods section (refer section 2.5) [30]. Among the potential multitarget (EGFR1, PI3Kinase and BRAF) allosteric inhibitors ZINC38783966, ZINC01456629 and ZINC01456628, the ligand binding affinity of ZINC38783966: (1S,2S)-1,2-Bis(1H-benzo[f]benzimidazol-2-yl) ethane-1,2-diol, was evaluated using molecular dynamics simulation studies in EGFR1 (6DUK), PI3Kinase (4A55) and (6P3D).

The RMSD graph in the dynamics analysis shows the root mean standard deviation for protein and ligand heavy atoms in the current frame with respect to the original frame. RMSD analysis is useful in assessing the quality of reproduction of the docked binding pose by a computational method, such as docking. The RMSD of the EGFR1- ZINC38783966 complex and BRAF-ZINC38783966 showed deviation below 2A and that of PI3Kinase-ZINC38783966 complex was below 3A (Fig. 6A, 7A, & 8A).

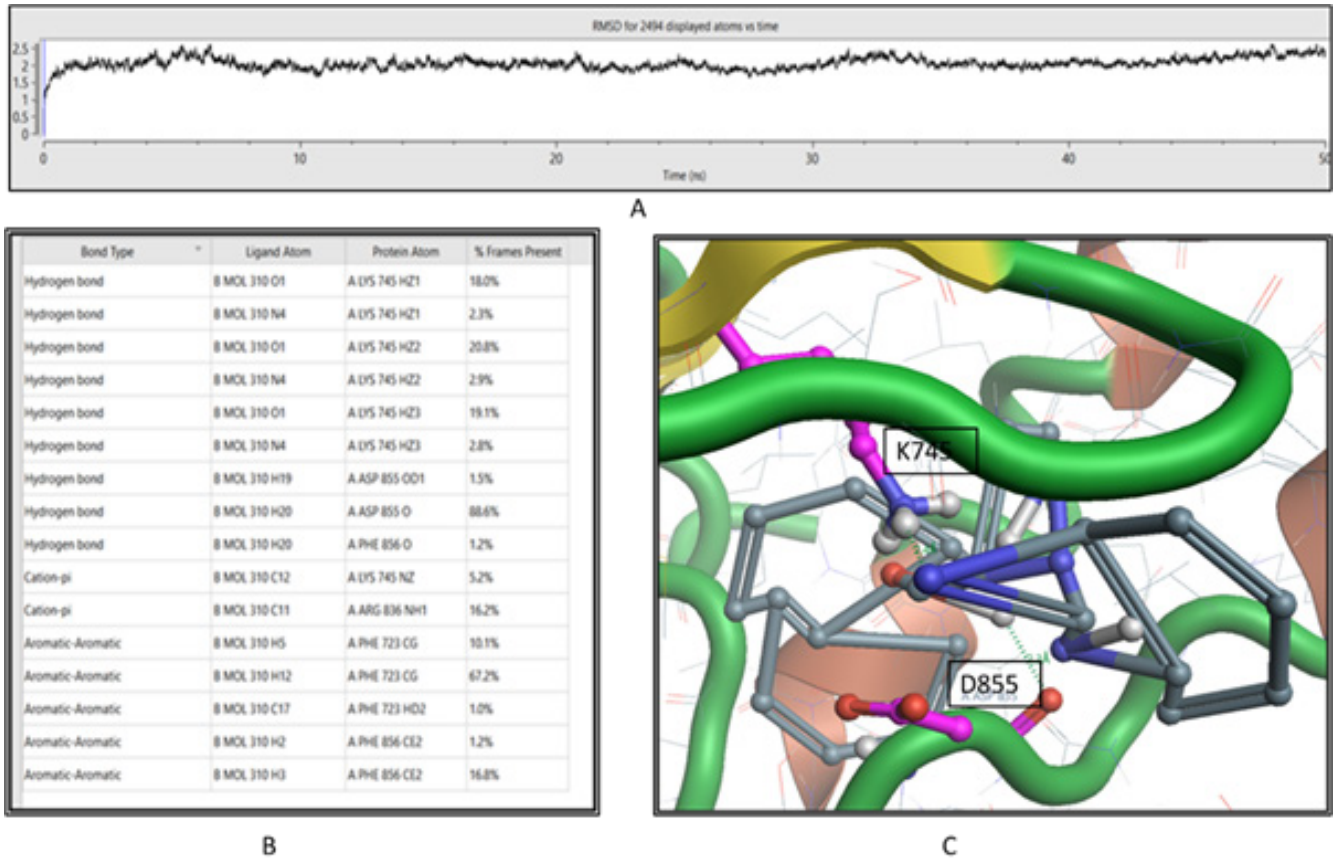

Figure 6 MD Studies on EGFR1 (6DUK) - ZINC38783966. A. represents the RMSD graph of the molecular dynamics simulation for 50ns. B. Represents the percentage of ligand contacts present in all frames of the trajectory. C. Represents the binding pose of ligand ZINC38783966 and the residues D855 and K745 of EGFR1 (6DUK) in hydrogen bond interaction.

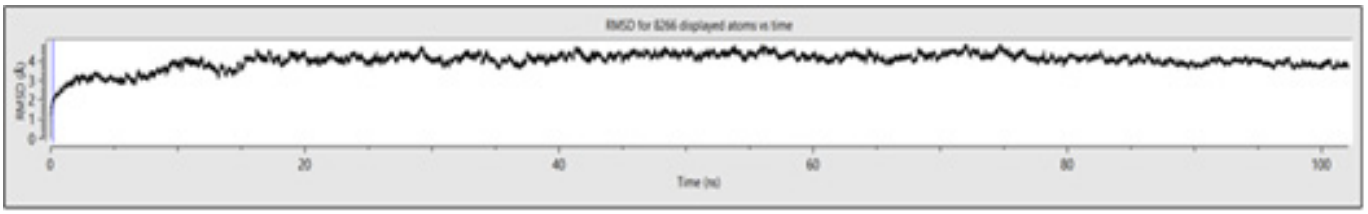

A

Bond Type	Ligand Atom	Protein Atom	% Frames Present
Hydrogen bond	B MOL 1012:...	A THR 909 O...	98.0%
Aromatic-Aromatic	B MOL 1012:...	A PHE 906 H...	14.7%
Aromatic-Aromatic	B MOL 1012:...	A PHE 906 H...	10.9%
Aromatic-Aromatic	B MOL 1012:...	A PHE 906 C...	45.8%
Aromatic-Aromatic	B MOL 1012:...	A PHE 906 C...	56.2%
Aromatic-Aromatic	B MOL 1012:...	A PHE 912 H...	12.7%
Aromatic-Aromatic	B MOL 1012:...	A PHE 912 H...	66.6%
Aromatic-Aromatic	B MOL 1012:...	A PHE 912 H...	13.0%
Aromatic-Aromatic	B MOL 1012:...	A PHE 929 H...	4.6%
Aromatic-Aromatic	B MOL 1012:...	A PHE 929 H...	23.3%
Aromatic-Aromatic	B MOL 1012:...	A PHE 929 HZ	22.2%
Aromatic-Aromatic	B MOL 1012:...	A PHE 929 H...	3.7%
Aromatic-Aromatic	B MOL 1012:...	A PHE 929 H...	15.0%
Aromatic-Aromatic	B MOL 1012:...	A PHE 932 H...	2.1%
Aromatic-Aromatic	B MOL 1012:...	A PHE 932 H...	3.2%
Aromatic-Aromatic	B MOL 1012:...	A TYR 937 CE1	2.0%
Aromatic-Aromatic	B MOL 1012:...	A TYR 937 CE1	8.0%
Aromatic-Aromatic	B MOL 1012:...	A PHE 991 C...	69.6%

B

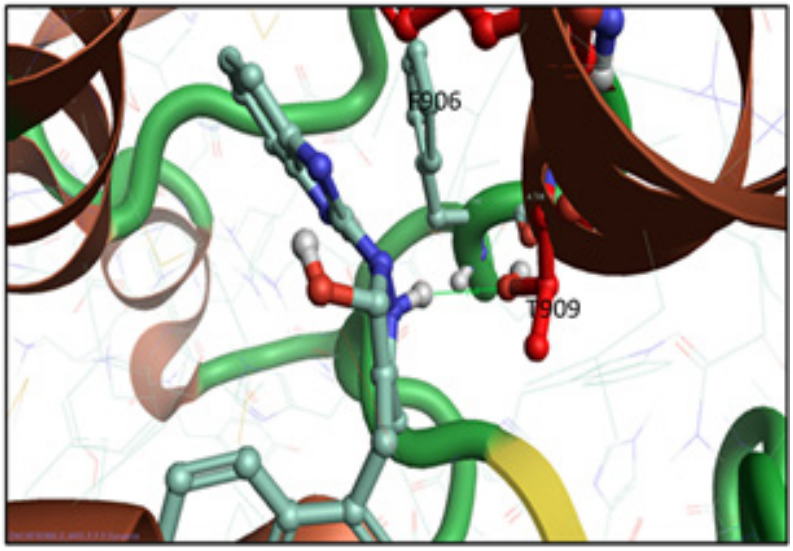

C

Figure 7 MD Studies on PI3Kinase (4A55)- ZINC38783966. A. Represents the RMSD graph of the molecular dynamics simulation for 100ns. B. Represents the percentage of ligand contacts present in all frames of the trajectory. C. Represents the binding pose of ligand ZINC38783966 and the residues T909 of PI3Kinase (4A55) in hydrogen bond interaction.

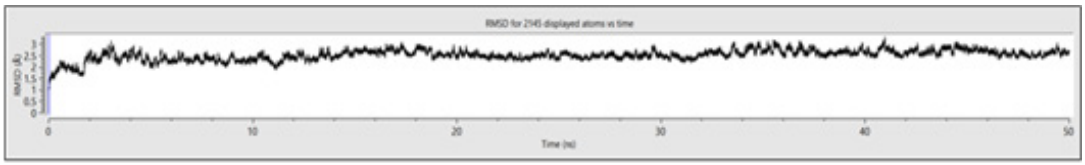

A

Bond Type	Ligand Atom	Protein Atom	% Frames Present
Hydrogen bond	B MOL 269 H20	A GLU 501 OE1	2.5%
Hydrogen bond	B MOL 269 H20	A GLU 501 OE2	31.9%
Hydrogen bond	B MOL 269 H18	A GLU 501 OE2	30.7%
Hydrogen bond	B MOL 269 H19	A ASP 594 OD1	25.1%
Hydrogen bond	B MOL 269 H19	A ASP 594 OD2	19.9%
Hydrogen bond	B MOL 269 H20	A ASP 594 O	3.0%
Cation-pi	B MOL 269 C16	A LYS 483 NZ	12.6%
Cation-pi	B MOL 269 C7	A HIS 574 NE2	2.0%
Cation-pi	B MOL 269 C13	A HIS 574 NE2	13.4%
Cation-pi	B MOL 269 C7	A ARG 575 NH2	1.4%
Aromatic-Aromatic	B MOL 269 H7	A HIS 574 ND1	12.6%
Aromatic-Aromatic	B MOL 269 H2	A HIS 574 ND1	5.1%
Aromatic-Aromatic	B MOL 269 C7	A HIS 574 ND1	4.3%
Aromatic-Aromatic	B MOL 269 C13	A HIS 574 ND1	13.1%
Aromatic-Aromatic	B MOL 269 H9	A HIS 574 ND1	9.4%
Aromatic-Aromatic	B MOL 269 H6	A HIS 574 ND1	4.3%

B

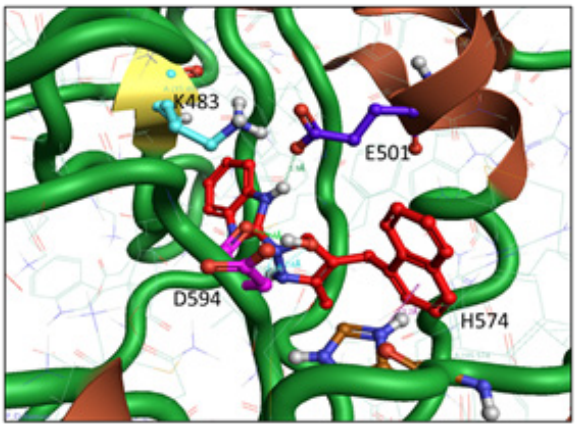

C

Figure 8 MD Studies on BRAF (6P3D) - ZINC38783966. A. Represents the RMSD graph of the molecular dynamics simulation for 50ns. B. Represents the percentage of ligand contacts present in all frames of the trajectory. C. Represents the binding pose of ligand ZINC38783966 and the residues T909 of BRAF (6P3D) in hydrogen bond interaction.

Protein Ligand Contacts: Allostery in proteins is a phenomenon where ligand binding at a distant place alters ligand binding at catalytic site. Theoretical and experimental studies have proved that allostery can be communicated through altered slow relaxation protein dynamics without any conformational change and can be related to evolution of ligand- binding site. Analysis of protein ligand complex during the entire trajectory provides the understanding of the ligand stability within the binding pocket based on the percentage of key residue contacts in the number of frames during the entire trajectory. The docked pose of EGFR1-ZINC38783966 pose. The residue D855 of DFG motif formed hydrogen bonding in more with the ligand in 88% of frames, while the residue K745 was observed to interact with the ligand in more than 60% of frames. The conserved K745-E762 salt bridge is also important in regulating αC-helix movement important for transition between active and inactive state of kinase domain. The residue K745 is a part of the conserved K745-E762 salt bridge that is also important in regulating αC-helix movement important for transition between active and inactive state of kinase domain. While the amino acid residue F723 showed aromatic- aromatic interaction in 67.2% of frames. D855 is a part of DFG motif, which plays key role in regulating kinase activity. The OH group of pyrazole in the ligand showed hydrogen bond interaction with aspartate residue of DFG motif in EGFR1 and BRAF (Fig. 4B, C). In the docked pose of PI3K - ZINC38783966, T909 formed Hydrogen bond in 99 % of frames. While the residues F906, F912, F829, F991 showed aromatic-aromatic interactions (Fig 5B, C). Analysis of protein ligands during the entire trajectory indicates whether key residue contacts are retained during entire trajectory. As was seen in the docked pose of BRAF - ZINC38783966 pose. The residues E501, D594 was engaged in hydrogen bonding interaction in more than 60% and 45% of frames. Only H574 showed aromatic- aromatic interaction during 50ns trajectory (Fig.6B, C). The movie of the molecular dynamics simulation study of the ligand ZINC38783966 with EGFR1 (6DUK, PI3Kinase (4A55) and BRAF (6P3D) (Supplementary material M1, M2 & M3).

Among the potential ligands from Pubchem ligands, the docked complex of compound 137352549 (2-[5-[2-(6-amino-3-pyridinyl) ethynyl]-4-methyl-3-oxo-1H-isoindol-2-yl]-2-(5-fluoro-2-hydroxyphenyl)-N-(2-thiazolyl) acetamide) with EGFR1, PI3Kinase and BRAF was subjected to molecular dynamics simulation study for 50ns. The RMSD graph during entire trajectory in the three complexes equilibrated towards the end of trajectory below 2 A (9A, 10A & 11A). Protein ligand contacts of EGFR1-

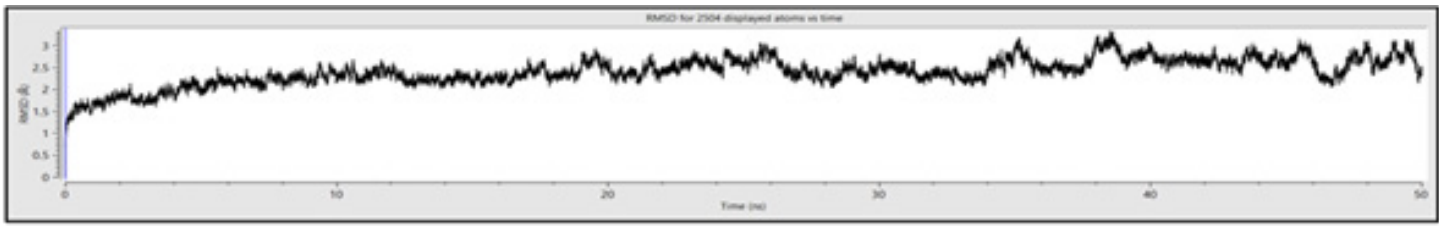

A

Contacts for 50 ns of the simulation between 0 ns and 50 ns

Bond Type	Ligand Atom	Protein Atom	% Frames Present
Hydrogen bond	B MOL 309 H1	A PHE 856 O	99.2%
Aromatic-Aromatic	B MOL 309 H15	A PHE 856 CE2	89.2%
Hydrogen bond	B MOL 309 H2	A ASP 855 OD1	34.0%
Hydrogen bond	B MOL 309 H2	A ASP 855 OD2	16.9%
Hydrogen bond	B MOL 309 H3	A GLU 865 OE1	10.0%
Hydrogen bond	B MOL 309 H3	A GLU 865 OE2	9.0%
Hydrogen bond	B MOL 309 H4	A GLU 865 OE1	10.2%
Hydrogen bond	B MOL 309 H4	A GLU 865 OE2	12.0%
Hydrogen bond	B MOL 309 H5	A GLU 865 OE1	6.4%
Hydrogen bond	B MOL 309 H5	A GLU 865 OE2	6.3%
Salt Bridge	B MOL 309 N4	A GLU 749 OE1	6.3%
Salt Bridge	B MOL 309 N4	A GLU 865 OE1	25.4%
Salt Bridge	B MOL 309 N4	A GLU 865 OE2	25.6%
Hydrogen bond	B MOL 309 O1	A LYS 745 HZ1	29.8%
Hydrogen bond	B MOL 309 O1	A LYS 745 HZ2	31.6%
Hydrogen bond	B MOL 309 O1	A LYS 745 HZ3	34.6%
Sulfur-lone Pair	B MOL 309 S1	A THR 854 OG1	24.9%
Sulfur-lone Pair	B MOL 309 S1	A ASP 855 OD1	74.5%
Sulfur-lone Pair	B MOL 309 S1	A ASP 855 OD2	33.2%

B

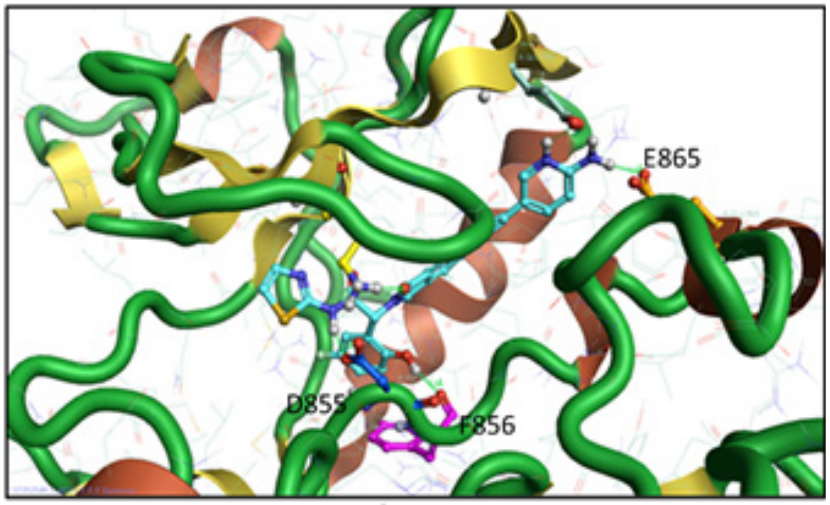

C

Figure 9 MD Studies on EGFR1 (6DUK) - 137352549. A. represents the RMSD graph of the molecular dynamics simulation for 50ns. B. Represents the percentage of ligand contacts present in all frames of the trajectory. C. Represents the binding pose of ligand 137352549 and the residues D855, F856 and E865 of EGFR1 (6DUK) in hydrogen bond interaction.

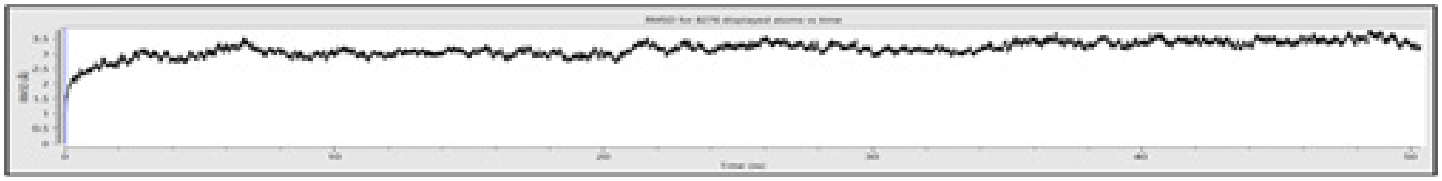

A

Contacts for 50 ns of the simulation between 0 ns and 50 ns

Bond Type	Ligand Atom	Protein Atom	% Frames Present
Sulfur-lone Pair	B MOL 1012 S1	A THR 1005 O	57.5%
Hydrogen bond	B MOL 1012 H4	A ILE 865 O	5.2%
Hydrogen bond	B MOL 1012 H3	A GLN 933 OE1	78.2%
Hydrogen bond	B MOL 1012 N3	A GLN 933 HE22	91.4%
Hydrogen bond	B MOL 1012 H2	A ASN 996 OD1	9.5%
Hydrogen bond	B MOL 1012 O1	A ASN 996 HD22	6.6%
Hydrogen bond	B MOL 1012 O3	A ASN 996 HD22	49.1%
Hydrogen bond	B MOL 1012 H4	A HIS 1000 O	7.8%
Hydrogen bond	B MOL 1012 H5	A HIS 1000 O	32.6%
Aromatic-Aromatic	B MOL 1012 C24	A PHE 861 HD1	91.3%
Aromatic-Aromatic	B MOL 1012 C6	A PHE 861 HE2	7.0%
Aromatic-Aromatic	B MOL 1012 H18	A PHE 906 CG	57.5%
Aromatic-Aromatic	B MOL 1012 C6	A PHE 906 HD1	29.3%
Aromatic-Aromatic	B MOL 1012 C23	A PHE 929 HE1	43.6%
Aromatic-Aromatic	B MOL 1012 C23	A PHE 929 HZ	40.8%
Aromatic-Aromatic	B MOL 1012 H15	A PHE 991 CG	24.6%

B

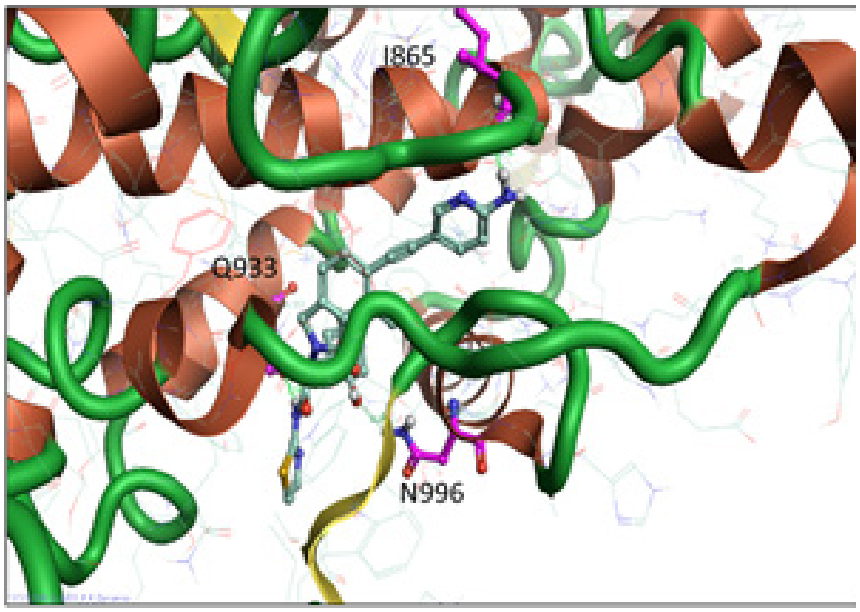

C

Figure 10 MD Studies on PI3KINASE (4A55) - PUBCHEM 137352549 A. represents the RMSD graph of the molecular dynamics simulation for 50ns. B. Represents the percentage of ligand contacts present in all frames of the trajectory. C. Represents the binding pose of ligand 137352549 and the residues I865, N996 and Q933 of PI3KINASE (4A55) in hydrogen bond interaction.

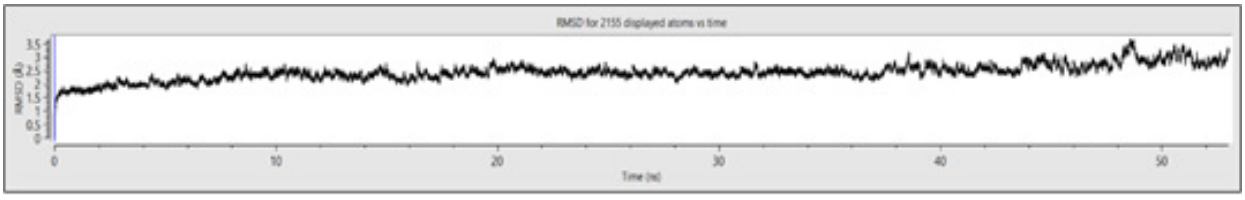

A

Bond Type	Ligand Atom	Protein Atom	% Frames Present
Sulfur-lone Pair	B MOL 269 S1	A HIS 574 O	22.1%
Sulfur-lone Pair	B MOL 269 S1	A ASP 594 OD2	5.6%
Hydrogen bond	B MOL 269 H5	A ALA 481 O	5.9%
Hydrogen bond	B MOL 269 H4	A ILE 527 O	73.5%
Hydrogen bond	B MOL 269 H5	A THR 529 OG1	80.8%
Cation-pi	B MOL 269 C25	A LYS 483 NZ	19.7%
Cation-pi	B MOL 269 C19	A ARG 575 NE	43.7%
Cation-pi	B MOL 269 C19	A ARG 575 NH1	8.8%
Cation-pi	B MOL 269 C19	A ARG 575 NH2	7.9%
Aromatic-Aromatic	B MOL 269 C19	A PHE 468 HZ	5.3%
Aromatic-Aromatic	B MOL 269 H20	A PHE 595 CG	38.8%

B

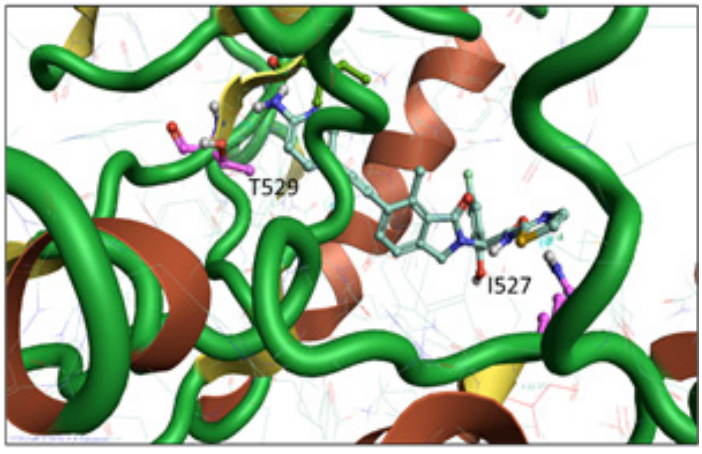

C

Figure 11 MD Studies on BRAF (6P3D) - PUBCHEM 137352549 MD A. represents the RMSD graph of the molecular dynamics simulation for 50ns. B. Represents the percentage of ligand contacts present in all frames of the trajectory. C. Represents the binding pose of ligand 137352549 and the residues I527 and T529 of BRAF (6P3D) - in hydrogen bond interaction..

137352549 shows that F856 of the 6DUK was able to interact with the F856, 99.2% of times D855 and E865 for approximately 50% of the times and K745 more than 99% with hydrogen bond. F856 showed aromatic-aromatic interaction with ligand in 89% of frames (Fig. 6B). Amino group of pyridines with E865, and E749, amide group of thiazoyl acetamide interacted with D855. Hydroxy group of isoindol interacted with K745 and OH group of hydroxy phenyls with F856 (99%) (Fig.7B & 7C). Ligand contacts in PI3Kinase – 137352549 2-[5-[2-(6-amino-3-pyridinyl) ethynyl]-4-methyl-3-oxo-1H-isoindol-2-yl]-2-(5-fluoro-2-hydroxyphenyl)-N-(2-thiazolyl) acetamide complex showed that the NH of pyridine and amino group of pyridine forms hydrogen bond with K-α helix I913 (Fig. 8A & B). MDS of BRAF Kinase with 137352549: 2-[5-[2-(6-amino-3-pyridinyl) ethynyl]-4-methyl-3-oxo-1H-isoindol-2-yl]-2-(5-fluoro-2-hydroxyphenyl)-N-(2-thiazolyl) acetamide (Fig. 9A &B). The movie of the molecular dynamics simulation study of the ligand 137352549 with EGFR1 (6DUK), PI3Kinase (4A55) and BRAF Kinase (6P3D) (Supplementary material M4, M5 & M6).

Increased levels of the tyrosine kinases and/or cognate ligands is common occurrence in different cancer types. Among various tyrosine kinases, EGFR1 has been under intense investigation due to proven role in multiple cancers. The drugs targeting EGFR1 have been useful in treating patients with cancer and manageable toxicity in comparison to chemotherapy, the treatment had limited or no benefit to patients after some time due to drug resistance. Studies have attributed drug resistance to mutations, gene amplification and activation of several downstream signalling pathways. Among these signalling pathways, PI3K/Akt/mTOR pathway and RAS/RAF/MEK/ERK (MAPK) alteration was mainly related to EGFR1 activation and interestingly, these pathways were also related to the development of resistance to chemotherapy (Granville et al., 2006). Importantly, PI3K/Akt/mTOR pathway was proved to be essential for growth of cancer cells in acidic or hypoxic conditions. One advantage was that the targeted therapy of PI3K/Akt/mTOR pathway resulted in inhibition of pathways in cancer cell (Granville et al., 2006). Further it was also proposed that inhibition of certain components of the PI3K/Akt/mTOR pathway may also be useful in stopping the growth of cancer or sensitize cancer cell for chemotherapy. However, the toxic side effects of inhibition of this pathway, like hyperglycaemia forced the researchers to develop a strategy where the pathway is targeted at multiple sites and related pathways. RAS–RAF–MEK–ERK signalling pathway (ERK signalling) are normally activated by receptor tyrosine kinase signalling. It further activates RAF proteins and triggers a cascade of the downstream kinases, finally leading to cellular effects (Lavoie et al., 2015). BRAF mutations were observed in various cancers varying from 9% in all cancers and 50% in melanoma. Mutated BRAFV600E can activate ERK signalling independent of RAS as an active monomer. However, there are only three approved BRAF inhibitors Vemurafenib, Dabrafenib, and Encorafenib for BRAFV600E metastatic melanoma. However, despite being potent inhibitors, the efficacy is short lived due to drug resistance thereby giving patients only short-term improvement. One of the important mechanisms of clinical resistance mechanisms of BRAF is the reactivation of receptor tyrosine kinases [31].

Thus, the results of the present investigation have identified novel molecules with multitarget inhibition potential targeting oncogenic targets EGFR1, PI3 kinase and BRAF kinase as single agent. However, these allosteric inhibitors may be used along with drugs to achieve an synergic effect binding at allosteric sites. Since the identified molecules shared the similarity to recent allosteric inhibitor JBJ-04-125-02 and the SwissADME evaluation of drug likeness was comparable to the inhibitors in the crystal structure complex, the molecules identified in this study stands good chance for their application in cancer therapy overcoming drug resistance. There is an urgent need to evaluate these compounds experimentally, based on the results of the present study.

Conclusion

Kinase inhibitors are successful in the therapy of cancer as they could specifically target only malignant cells, thereby reducing the side effects tremendously. However, the major drawback is that these drugs lose their efficacy due to drug resistance. Overcoming drug resistance requires novel drug discovery and approval and is time consuming, resulting in the suffering of many patients, leaving them with few treatment options. In conclusion, we described the discovery of multi-target inhibitors as a novel inhibitor of three important targets namely EGFR1, PI3Kinase and BRAF. Further, it has identified novel potential multitarget -allosteric inhibitors that can target important checkpoints of the signal transduction pathways namely PI3K/Akt/mTOR and RAS/RAF/MEK/ERK (MAPK). The discovery could lead to the development of new mutant resistant potential inhibitors, as the study focused on the triple mutant structure of EGFR1 (6DUK) and the mutant structure of BRAF (6P3D).

Declarations

Funding

The corresponding author is pleased to acknowledge department of science & technology, Government of India for financial support vide reference no SR/LS310/2017 under Women Scientist Scheme to carry out this work.

Conflicts of interest/Competing interests: None.

Acknowledgements

The corresponding author is pleased to acknowledge the department of science & technology, Government of India for financial support vide reference no SR/LS310/2017 under Women Scientist Scheme to carry out this work. The authors would like to thank Cresset for providing the software to carry out this work. The authors would also like to thank Prof. P.P. Reddy, the Research Director at Bhagwan Mahavir Medical Research Centre, as well as the Management, for their ongoing encouragement and support

References

1 AACR project GENIE: Powering precision medicine through an international consortium. (2017). Cancer Discovery. 7: 818-831

2 Agianian B, Gavathiotis E. (2018) Current insights of BRAF inhibitors in cancer. Journal of Medicinal Chemistry. 61: 5775-5793.

3 Baell JB, Holloway GA. (2010). New substructure filters for removal of pan assay interference compounds (PAINS) from screening libraries and for their exclusion in bioassays. Journal of Medicinal Chemistry. 53: 2719-2740.

4 Bardelli A. (2003). Mutational analysis of the tyrosine Kinome in colorectal cancers. Science. 300: 949-949.

5 Bartram CR, De Klein A, Hagemeijer A, Van Agthoven T, Van Kessel A G, et al. (1983). Translocation of C-abl oncogene correlates with the presence of a Philadelphia chromosome in chronic myelocytic leukaemia. Nature. 306: 277-280.

6 Bauer MR, Mackey MD. (2019). Electrostatic complementarity as a fast and effective tool to optimize binding and selectivity of protein–ligand complexes. Journal of Medicinal Chemistry. 62: 3036-3050.

7 Bendell JC, Rodon J, Burris HA, De Jonge M, Verweij J, et al. (2012). Phase I, dose-escalation study of BKM120, an oral pan-class I PI3K inhibitor, in patients with advanced solid tumors. Journal of Clinical Oncology. 30: 282-290.

8 Bhullar K S, Lagarón NO, McGowan EM, Parmar I, Jha A, et al. (2018). Kinase-targeted cancer therapies: Progress, challenges and future directions. Molecular Cancer, 17: p. 48.

9 Brenk R, Schipani A, James D, Krasowski A, Gilbert I, et al. (2008). Lessons learnt from assembling screening libraries for drug discovery for neglected diseases. ChemMedChem. 3: 435-444.

10 Caballero J, Alzate-Morales JH. (2012). Molecular dynamics of protein kinase-inhibitor complexes: a valid structural information. Curr. Pharm. Des. 18: 2946–2963.

11 Chalhoub N, Baker SJ. (2009). PTEN and the PI3-kinase pathway in cancer. Annual Review of Pathology: Mechanisms of Disease. 4: 127-150.

12 Cheeseright T, Mackey M, Rose S, Vinter A. (2006). Molecular Field extrema as descriptors of biological activity: Definition and validation. Journal of Chemical Information and Modeling. 46: 665-676.

13 Chong ZZ, Shang YC, Wang S, Maiese K. (2012). A critical kinase Cascade in neurological disorders: PI3K, Akt and mTOR. Future Neurology. 7: 733-748.

14 Cotto-Rios XM, Agianian B, Gitego N, Zacharioudakis E, Giricz O, et al. (2020). Inhibitors of BRAF dimers using an allosteric site. Nature Communications, 11: 4370

15 Daina A, Michielin O, Zoete V. (2017). SwissADME: A free web tool to evaluate pharmacokinetics, drug-likeness and medicinal chemistry friendliness of small molecules. Scientific Reports. 7: 42717

16 Degirmenci U, Wang M, Hu J. (2020). Targeting aberrant ras/RAF/Mek/Erk signaling for cancer therapy. Cells, 9: p. 198.

17 Eastman P, Swails J, Chodera JD, McGibbon RT, Zhao Y, et al. (2017). OpenMM 7: Rapid development of high performance algorithms for molecular dynamics. PLOS Computational Biology. 13: e1005659.

18 Egan WJ, Merz KM, Baldwin JJ. (2000). Prediction of drug absorption using multivariate statistics. Journal of Medicinal Chemistry. 43: 3867-3877.

19 Endres NF, Barros T, Cantor AJ, Kuriyan J. (2014). Emerging concepts in the regulation of the EGF receptor and other receptor tyrosine kinases. Trends in Biochemical Sciences. 39: 437-446.

20 Forbes SA, Bindal N, Bamford S, Cole C, Kok CY, et al. (2010). COSMIC: Mining complete cancer genomes in the catalogue of somatic mutations in cancer. Nucleic Acids Research. 39: D945-D950.

21 Futreal PA, Coin L, Marshall M, Down T, Hubbard T, et al. (2004). A census of human cancer genes. Nature Reviews Cancer. 4: 177-183.

22 Gabelli SB, Echeverria I, Alexander M, Duong-Ly KC, Chaves-Moreira D, et al. (2014). Activation of PI3Kα by physiological effectors and by oncogenic mutations: Structural and dynamic effects. Biophysical Reviews. 6: 89-95.

23 Gagic Z, Ruzic D, Djokovic N, Djikic T, Nikolic K. (2020). In silico methods for design of kinase inhibitors as Anticancer drugs. Frontiers in Chemistry. 7: p. 873

24 Gan HK, Cvrljevic AN, Johns TG. (2013). The epidermal growth factor receptor variant III (EGFR1vIII): Where wild things are altered. FEBS Journal. 280: 5350-5370.

25 Garuti L, Roberti M, Bottegoni G. (2015). Multi-kinase inhibitors. Current Medicinal Chemistry. 22: 695-712.

26 Ghose AK, Viswanadhan VN, Wendoloski JJ. (1999). A knowledge-based approach in designing combinatorial or medicinal chemistry libraries for drug discovery. 1. A qualitative and quantitative characterization of known drug databases. Journal of Combinatorial Chemistry. 1: 55-68.

27 Granville CA, Memmott RM, Gills JJ, Dennis PA. (2006). Handicapping the race to develop inhibitors of the Phosphoinositide 3-Kinase/Akt/Mammalian target of Rapamycin pathway. Clinical Cancer Research. 12: 679-689.

28 Kittler H, Tschandl P. (2018). Driver mutations in the mitogen-activated protein kinase pathway: The seeds of good and evil. British Journal of Dermatology. 178: 26-27.

29 Knighton DR, Zheng JH, Ten Eyck LF, Ashford VA, Xuong NH, et al. (1991). Crystal structure of the catalytic subunit of cyclic adenosine monophosphate-dependent protein kinase. Science 253: 407–414.

30 Koes DR, Camacho CJ. (2012). ZINCPharmer: Pharmacophore search of the ZINC database. Nucleic Acids Research. 40: W409-W414.

31 Kostler WJ, Zielinski CC. (2014). Targeting receptor tyrosine kinases in cancer. Receptor Tyrosine Kinases: Structure, Functions and Role in Human Disease. p.225-278.